DTU Library

# Subpolar gyre and temperature drive boreal fish abundance in Greenland waters

**Post, Søren; Werner, Karl Michael; Núñez-Riboni, Ismael; Chafik, Léon; Hátún, Hjálmar; Jansen, Teunis**

*Published in:*
Fish and Fisheries

*Link to article, DOI:*
10.1111/faf.12512

*Publication date:*
2021

*Document Version*
Peer reviewed version

# Subpolar gyre and temperature drive boreal fish abundance in Greenland waters

Søren Post[1,2], Karl-Michael Werner[3], Ismael Núñez-Riboni[3], Léon Chafik[4], Hjálmar Hátún[5], Teunis Jansen[1,2]

[1]GINR – Greenland Institute of Natural Resources, Nuuk, Greenland

[2]DTU Aqua – National Institute of Aquatic Resources, Lyngby, Denmark

[3]Thünen Institute of Sea Fisheries, Bremerhaven, Germany

[4] Department of Meteorology and Bolin Centre for Climate Research, Stockholm University, Stockholm, Sweden

[5]Faroe Marine Research Institute, Tórshavn, Faroe Islands

Corresponding author: Søren Post; GINR – Greenland Institute of Natural Resources, Nuuk, Greenland*; Tel.: +299 361200; E-mail address: sopo@natur.gl.*

Keywords: *environmental drivers, GAM, lagged response, Irminger- Labrador Seas, trawl survey, water density.*

## Abstract

As result of ocean warming, marine boreal species shift distribution poleward and increase in abundance at higher latitudes. A key to predict the impact of warming on these species is to disentangle the roles of anthropogenically induced climate change and natural variability. Scattered field observations in the first half of the 20th century suggested that boreal fish may coherently invade Greenland waters when temperatures rise, but this hypothesis has remained untested. Therefore, we studied how local temperature variability and the dynamics of the subpolar gyre, a large-scale driver of oceanic conditions in the North Atlantic, affect abundance of boreal fishes in a region that sharply defines their lower thermal boundary. We analysed information from demersal trawl surveys from 1981-2017 for species distributed from shallow shelf regions to depths of 1500 m collected at over 10,000 stations along ~ 3000 km of the coast of Greenland. Our results show that local temperature and variability of Labrador and Irminger Sea water in the subpolar gyre region drive interdecadal variability of boreal fish abundance in Greenland waters. Although temperature fluctuations were higher in shallow than deep regions, fish abundance changed as quickly in great depths as in shallow depths. This link between physics and biology provides an opportunity for prediction of future trends, which is of utility in Greenland, where fisheries constitute more than 90% of the national export value.

## Table of Contents

## 1. Introduction

Fish distribution and abundance change in response to rising temperatures (Hastings et al., 2020; Perry, Low, Ellis, & Reynolds, 2005; Simpson et al., 2011). In Arctic and subarctic regions, global warming is estimated to happen faster than the global average and ecosystems are predicted to change faster than anywhere else (Fossheim et al., 2015; IPCC, 2019). Here, where boreal fishes face their lower thermal threshold, abundance is particularly sensitive to changes in temperature (Fossheim et al., 2015; Fredston-Hermann, Selden, Pinsky, Gaines, & Halpern, 2020; Kortsch et al., 2015). While boreal species are predicted to invade arctic and arcto-boreal ecosystems, cold-water adapted specialists might face declining habitat suitability, increasing competition and potentially extinctions (Cheung et al., 2009; Christiansen, Mecklenburg, & Karamushko, 2014; Dahlke et al., 2018; Fossheim et al., 2015). Greenland waters encompass several climatic zones and border the Irminger Sea and the Labrador Sea (Figure 1). Off the east coast, in the central Irminger Sea, warm and salty Atlantic water dominates the surface waters (Figure 1). These surface waters protrude onto the East Greenland shelf, where they face the cold and fresh southward-flowing East Greenland current (Våge et al., 2011). As consequence, suitable conditions for boreal species can mainly be found in eastern and southern Greenland, where Atlantic water masses dominate the environmental regime (Jørgensen, Hvingel, & Møller, 2015; Riget et al., 2000).

In the subpolar North Atlantic, water characteristics such as temperature, salinity, and density are intrinsically linked to volume and distribution of mode waters (Figure 1). Mode waters are water masses with identifiable relatively uniform properties of large volumes (Speer & Forget, 2013). Boundaries between these mode waters are associated with large density gradients and thus the main current systems. Variable air-sea forcing over the North Atlantic (e.g. North Atlantic Oscillations (NAO)) drives water formation (convection) (Häkkinen & Rhines, 2004) modifies the properties and distribution of mode waters. The associated deep-reaching density anomalies are reflected as changes in the sea surface height through the steric relation (Gill & Niller, 1973). The subpolar gyre (SPG) index, which is calculated from the sea surface height field (Hátún & Chafik, 2018), thus represents the principal changes in the mode waters and reflects fundamental aspects of the marine climate in the North Atlantic. The variability represented by the gyre index has its centre of action in the western Irminger Sea and along a swath around the southern tip of Greenland and into the Labrador Sea (Figure 1). The concept of the SPG index as a single time series can, however, not adequately represent the conditions in the Irminger and Labrador Seas. A recent analysis shows that the gyre dynamics are split in two so-called principal components, which reflect water density properties in the subpolar North Atlantic (Hátún & Chafik, 2018). The first principal component reflects the slow variability in the deep waters in the Labrador Sea, extending into the western Irminger Sea – the Western Mode Water (WMW) (Figure 1), while the second principal component represents the stronger interannual variability of the lighter mode water classes between the

Rockall plateau and the eastern Irminger Sea – the Eastern Mode Water (EMW) (Hátún & Chafik, 2018) (Figure 1).

The strength of the SPG affects concentration of nutrients (Hátún, Somavilla, Rey, Johnson, & Mathis, 2017; Johnson, Inall, & Häkkinen, 2013) and abundance and distribution of zooplankton, fish and marine mammals (Hátún et al., 2016, 2009; Núñez-Riboni et al., 2013; Pedchenko, 2005). Yet, these biological links related to the SPG have been described almost solely in the eastern and central part of the gyre (the Rockall plateau, the Faroese and Icelandic waters), and information about how the SPG affects ecosystems around Greenland is still scarce.

Anecdotal and scattered information from the early 20$^{th}$ century suggest that abundance of pelagic and demersal boreal fish increases in Greenland waters, when temperatures rise (Hansen, 1949; Jensen & Hansen, 1931; Tåning, 1948). However, this is limited to qualitative (e.g. "high" or "low" abundance) descriptions. For the majority of non-target species in Greenland waters and in contrast to other arctic-boreal ecosystems, such as the Barents Sea, sensitivity to temperature has not been quantitatively tested and recent reviews must still rely on information based on observations from the early 20th century (Drinkwater, 2006; Drinkwater & Kristiansen, 2018). Yet, information about how fish abundance responds to environmental change is necessary to lay the foundation to predict fish distribution in the future and draw conclusions on socio-ecological implications of rising temperatures.

Over the past years, increasing amounts of evidence have shown that marine biota in the subpolar North Atlantic are regulated by the SPG. This suggests that water densities in the Irminger and Labrador Seas, local temperature and fish abundance could covary in shelf and slope regions in offshore Greenland waters. To test this hypothesis, we use observational data from 35 years of scientific fishery surveys covering shelf and slope regions from 40 to 1500 m depth to include often neglected slope and deep-sea species. We focus on boreal fish with low commercial exploitation rates to ensure that the population signals are only related to the environment. We firstly test if fish abundances correlate with physical properties (i.e. temperature, salinity and current speed) in Greenland shelf and slope areas and secondly investigate if water densities in the Labrador and Irminger Seas, which cover fundamental aspects of the oceanography in the study region, are a driving force of boreal fish abundance. We apply different statistical approaches and data transformations to investigate if high (e.g. interannual) or low-frequency (e.g. interdecadal) variability dominates correlations between fish abundance and environmental drivers. Lastly, we investigated if changes in the oceanic conditions precede the fish abundance.

## 2. Materials and methods

### 2.1. Fish data collection

More than 260 fish species have been documented in the Exclusive Economic Zone of Greenland (Møller et al., 2010), of which the majority is classified as boreal species (Mecklenburg et al., 2018). Data on fish abundance for 1981-2017 were collected during three annual bottom trawl surveys covering different regions, depths and periods: the German groundfish survey in Greenland waters conducted by the Thünen Institute of Sea Fisheries (1981-2017) and the Greenland shrimp and fish survey (2005-2017), as well as the Greenland Greenland halibut survey (1997-2017), both carried out by the Greenland Institute of Natural Resources (Figure 2, Supporting information Table S1) (Fock, 2016; Jørgensen, 2017; Retzel, 2017, 2019). Each survey is designed to monitor groundfish stocks and to serve the assumption that catches representatively cover groundfish composition and abundance. However, most species are not caught frequently, and some are targeted by large fisheries, which can mask signals from the environment. Prior to analysis, we therefore scanned the survey data to identify the species suitable for including in the study. This selection was conducted using a set of criteria: Firstly, a species should be present in at least 1% of the total number of stations. Secondly, using plots of their distributions, species were selected by visual inspection when they showed higher presence in East than in West Greenland and if classified as boreal in Mecklenburg *et al.* (2018). To focus on non-target species, we examined commercial fishery logbooks, which became available in 1997 as well as catch records for the whole time series. The commercially important species, Atlantic cod and redfish (*Sebastes* spp., Sebastidae), were excluded to avoid biases. Following these criteria, ten fish species were chosen for analysis: Atlantic wolffish (*Anarhichas lupus*, Anarhichadidae), blue ling (*Molva dipterygia*, Lotidae), blue whiting (*Micromesistius poutassou*, Gadidae), greater argentine (*Argentina silus*, Argentinidae), haddock (*Melanogrammus aeglefinus*, Gadidae), ling (*Molva molva*, Lotidae), roughhead grenadier (*Macrourus berglax*, Macrouridae), round ray (*Raja fyllae*, Rajidae), saithe (*Pollachius virens*, Gadidae) and tusk (*Brosme brosme*, Lotidae). Particular species, e.g. blue whiting and greater argentine, often occur pelagically and are not ideally sampled with bottom-trawls, which can result in non-representative sampling. However, bottom trawl surveys are accepted as valuable information in their stock assessments and also used for studying abundance trends of these species in other regions (Heino, Engelhard, & Godø, 2008; ICES, 2018b, 2018a) and we therefore decided to include them in the analysis. 1992 and 1994 were omitted due to poor survey coverage. For the Greenland shrimp and fish survey, only data from 2005 and later were used because the survey design changed in 2005, making potentially longer time series inconsistent. A description of the three surveys spatial overlap is given in Post *et al.* (2019). In total, observations from 10,373 trawl stations covering a shore distance of ~ 3000 km went into the analysis.

## 2.2. Fish abundance model

We used data from trawl surveys to model annual abundance indices, which we afterwards linked to environmental parameters. Prior modelling catch data, they were explored for outliers, heterogeneity of variance, normality, collinearity and independence following the protocol from Zuur *et al.* (2010). In order to standardize abundance and eliminate bias from uneven sampling effort, we applied Generalized Additive Models (GAMs) (Hastie & Tibshirani, 1986). GAMs have been broadly accepted for analysing ecological data including fish distribution and abundance (Berg, Nielsen, & Kristensen, 2014; Maunder & Punt, 2004; Wood, 2017) and suited our case with various nonlinear relationships between the observed numbers and the covariates. To develop the models we used an information theoretic approach (Burnham & Anderson, 2002), defining candidate models (based on biological knowledge) and fitting them to the observations. Observations were highly zero inflated (absence ranged from 47.8 - 98.7% across species) and overdispersed (with few outstandingly large catches). To overcome these challenges, we chose a negative binomial distribution for the observations, which has been applied successfully in other studies for modelling spatiotemporal fish distribution from zero inflated data (Irwin et al., 2013; Stenberg et al., 2015). Initially we also inspected a Tweedie distribution (Tweedie, 1984), which can also deal with some of the same issues but decided to use negative binomial distribution because of better model performance. To deal with the large heteroscedasticity typical of fish abundance data, a logarithmic link function between the predictors and response variable was chosen. Model fitting was done in R (R Core Team, 2018) using the *mgcv* package (Wood, 2017). In the full model prior model selection for every individual species, we assumed the following relationship between numbers of caught fish ($\mu$) at station *i* and the external factors:

$$\log(\mu_i) = \log(Swept\ area_i) + f(Axis_i) + f(Depth_i) + f(Time_i) + f(Day\ of\ year_i) + Survey_i + Year_i$$

where *Swept area* was an offset variable accounting for uneven sampling effort (Maunder & Punt, 2004). *Axis* (red line in Figure 2a) represented locations on a line following the coast on which fishing stations were assigned to by shortest distance and was used for describing the spatial distribution. *Depth, Time, Day of Year* and *Year* were their respective values, while *Survey* was one of the tree surveys used (Supporting information Table S2). For modelling the non-linear effects, smoothing functions $f$ () were used and for constructing these we largely followed Wood (2017). Thin plate regression splines were applied for f(*Axis*) and f(*Depth*) and a cyclic cubic regression spline for f(*Time*) and f(*Day of year*). Whenever interactions occurred, tensor product smoothers were used. A small value (k = 5) was chosen for the basis dimension k (related to the number of knots) for f(*Depth*), f(*Time*) and f(*Day of year*). This allowed for only few optima, which is a realistic representation of the dependence of fish abundance with these variables. For the case of f(*Axis*), there were no theoretical reasons to constrain k, and following suggestions from Wood (2017), it was chosen as large as the computation capabilities permitted (k = 100 in our case). This allowed for many hotspots along the coast. The final models for every species were selected by means of Akaike Information Criteria (AIC) (Akaike, 1974), using a backward selection procedure beginning with all covariates included and stepwise reduction.

## 2.3. Hydrography

The full-depth temperature, salinity and current velocity data are based on the global ocean reanalysis ORAS5 (ORAS5, 2019; Zuo, Balmaseda, Tietsche, Mogensen, & Mayer, 2019). The spatial resolution is 0.25 degree in latitude and longitude while the vertical resolution varies with depth, increasing from bottom towards surface (~1 m near surface and ~100 m at 1000 m depth). To inspect the correlations of fish abundance with temperature, salinity and current speed, we used the hydrography data from five areas along the coast (characterized by high fish densities) with 6 positions in each (bottom right inset in Figure 3), of which different bottom depths (200m, 300m, 400m, 1000m, 1500m and > 1500 m outside the shelf) were represented. To achieve data from positions as close as possible to these depths, we found positions that could be verified by trawl survey data. As a result, the positions were located in irregular patterns, i.e. not in straight transects. For the chosen positions, we calculated the average July-September value of each ORAS5 depth level for every year between 1981-2017. We then used the temperature from the depths having the highest (modelled) abundance for each species to correlate with the abundance index.

## 2.4. Subpolar gyre and water densities

Traditionally, the SPG index, which reflects variations of the gyre strength, has been calculated using altimetry data that is available since 1993 (Häkkinen & Rhines, 2004; Hátún & Chafik, 2018). However, as demonstrated in Hátún and Chafik (2018), the SPG strength can be successfully reconstructed from potential density anomaly referenced to 1000 dbar and averaged over the top 1000-m layer in the vicinity of the Reykjanes Ridge as calculated from the EN4 data set (1950-2018). This reconstruction is important since our aim is to examine the environmental conditions back to 1981, which would not have been possible using satellite altimetry only. Furthermore, we also use a second index reflecting predominantly the variability of deep convection in the Labrador Sea, an important indicator of the marine climate in the Subpolar North Atlantic. This index is reconstructed using potential density anomaly referenced to 2000 dbar and averaged between 1000 and 2500 m in the Labrador Sea. Thus, to capture the water mass variability in the SPG, we have constructed two different time series of the density anomalies at two separate regions, the Irminger Sea (Reykjanes Ridge, 0-1000m depth, 40-15°W, 55-65°N) and Labrador Sea (1000-2500m depth, 60-45°W, 55-65°N) using the EN4 data set (Good, Martin, & Rayner, 2013) with a bias correction method described in Gouretski & Reseghetti (2010). From now on these two indices are referred to as the Labrador Sea density (LD) and Reykjanes Ridge density (RD), which largely reflect the two first principal components calculated from satellite altimetry. The relationship between the two indices and temperatures of the central North Atlantic, including Greenland waters, is investigated through spatial correlations. Varying oceanic conditions during different SPG regimes were inspected through an analysis of the temperature field during anomalous periods of the density anomaly at four transects crossing some of the high fish abundance areas and central Seas.

### 2.5. Statistical tests

We used Spearman's rank correlation, a measure of the monotonic relationship between the variables, which does not require a linear relationship between covariates and observations to be normal distributed (Hauke & Kossowski, 2011; Spearman, 1904). Modelled trawl catch data were used as proxy for fish abundance. Inspections of the catches showed that not all species were caught in all years, despite consistent survey coverage. When testing correlations among abundance and other covariates, abundance index values for zero catch years were replaced with values equal to the lowest observed in the time series. We then tested the sensitivity of our results against this choice, by examining the difference between using with and without replacement of zeros. A significance threshold of 0.05 was set for the *p*-value. Autocorrelation in time series inflates the chance of getting type I errors (detecting significant relationships where none exist) (Pyper & Peterman, 1998). In order to account for this, the test procedure for significance of correlations was adjusted following Pyper and Peterman (1998, 2011) by reducing the effective number of degrees of freedom (increasing the p-values) according to the degree of autocorrelation. Running multiple correlation tests also inflates the change of getting type I errors. Hence, to examine if significant correlations could be an artefact of this, we calculated the amount of expected type I errors and the probability of achieving n+ positive correlations out of a total of N correlations analysis without any of these being true. The number of falsely significant correlations were assumed to be binomial distributed with the probability of success $p$=0.05/2. In order to gain insight if fish abundance and environmental drivers correlate stronger on high (e.g. interannual) or low-frequency (e.g. interdecadal) time scales, we compared correlation results from the default settings (explained above) with first-differenced and 3-year running mean abundance values (Pyper & Peterman, 1998). A first-differenced time series of abundance depicted as $\Delta\text{abundance}_{\text{year}} = \text{abundance}_{\text{year}} - \text{abundance}_{\text{year-1}}$ were used to investigate interannual changes, while the 3-year running mean for assessing low-frequency variations (Pyper & Peterman, 1998). Delayed relationships between environmental parameters and abundance were investigated by lagging environmental parameters compared to the abundance.

## 3. Results

### 3.1. Fish abundance in relation to temperature, salinity and current speed

Fish abundance models without interactions were selected for further analyses because these were the only models that fitted the observations adequately concerning residual patterns and did not show problematic edge effects. Minor differences in explanatory variables occurred between the individual species models (Supporting information Table S3). The final models explained 46-88% of the deviance in the data, with a mean of 69%.

For all species, abundance was low in the late 1980s and early 1990s and increased in the mid and late 1990s, which coincided with an increase in temperature (Figure 3). The only exception to this common pattern was Atlantic wolffish, which showed highest abundance in the late 1980s to the early 2000s. The amplitude of fluctuations in temperature differed across depths (Figure 3). Fish abundance followed fluctuations in temperature from shallow parts of the shelf (40 m) where temperature oscillated with ~3 °C over time, to deep regions of the slope (1200 m) where temperature did not fluctuate with more than ~0.5 °C (Figure 3). Temperature showed similar temporal trends across depths but decreased considerably stronger and quicker in deep regions than in shallow regions after 2010. Out of the ten species, seven were significantly or border-line significantly ($p < 0.053$) positively correlated with temperature. This is more than expected by random ($p < 0.001$, N = 10, $n^+ = 5$) (Table 1, Figure 3, and Supporting information Figure S1 and S2 for results on normal scale and with model uncertainties). The choice of using zero or the lowest observed value in years where the given species were not present in any samples did not change significance levels. Salinity showed positive correlations with abundance for two species and current speed with none (Table 1).

When testing low-frequency correlations (3 year running mean abundance) between abundance and temperature, significant correlations dropped to two species (Table 2). For the high-frequency changes (first differenced data), only Atlantic wolffish correlated significantly with temperature (Table 2). The correlation coefficients between lagged abundances and temperature were highest at lag zero and decreased with increasing lag years (Supporting information Table S4).

## 3.2. Fish abundance and the subpolar gyre

Both LD and RD increased in the 1980s and peaked in the early-mid 1990s coinciding with decreasing temperatures (Figure 3 and 4). They decreased again in the late 1990s until RD increased around 2006 and LD around 2013. Eight out of ten species were either significantly correlated with LD or RD (Table 1). LD and RD were significantly negative correlated with the abundance of seven and three species, respectively (Table 1). The probability of getting three type I errors was not significant ($p < 0.001$, N = 10, $n^+ = 3$). Low-frequency correlations (3 year running mean abundance) between abundance and LD and RD decreased compared to the default method (Table 2), but was still above what could be expected by random coincidences (LD, $p < 0.001$, N = 10, $n^+ = 5$; RD, $p = 1.64e^{-3}$, N = 10, $n^+ = 2$). For the high-frequency changes (first differenced data), two species correlated with RD and none with LD (Table 2).

As results from the default approach were considerably more similar to the low-frequent than to the high-frequent correlations, it appears that most of the variability in fish abundance is explained by decadal rather than annual fluctuations driven by the subpolar gyre (Table 2). The correlation coefficients between abundance and LD were highest without lag for most species and significant correlations peaked at lags between two and six years between abundance and RD (Supporting information Table S4 and Figure S3). The results thereby indicate that fish abundance shows a lagged relation to RD, and thereby properties of Eastern Mode Waters.

Temperature conditions east and south of Greenland were examined during high (1995), low (2007) and medium (2017) LD and RD (Figure 5). During high water densities (1995), less warm Atlantic water occurred in the Labrador and Irminger Seas and along the Greenland coast compared to low density (2007). More cold water of Arctic origin water was found close to the East Greenland coast early 90s, where it both extended further off the coast and reached deeper. Along the whole Labrador Sea transect, water below 3°C were considerably more present when LD and RD were higher. These observations illustrate that cold waters showed stronger presence in East and South Greenland, when water densities were high in the early 1990s. Horizontal correlation plots between the two SPG indices (LD and RD) and summer temperatures at different depths in the wider North Atlantic confirms this general negative correlation, especially along and on the Greenland shelf (Supporting information Figure S5). In the most recent period of the time series (2017), where RD was positive and LD negative, temperature in surface waters was slightly below the mid-2000s, but warmer than the 1990s. In the Ikermit transect, reflecting the Irminger Sea, the deeper waters are seen to be colder than in the 1990s and 2000s.

## 4. Discussion

Results of this study show that abundance of boreal fish covaries with local temperature and water density anomalies in offshore regions in the Labrador and Irminger Seas. These results are in line with previous findings that distribution and abundance of boreal species follows increasing temperatures in regions, where they encounter their lower thermal threshold (Fossheim et al., 2015; Fredston-Hermann et al., 2020). However, our results furthermore indicate that variation in Labrador- and Irminger Sea water formation is a better indicator than only temperature, salinity, or current speed, for describing the variation of fish abundance in this region. This leads to the conclusion that yet not all biogeographic implications of variability in the SPG are understood. The fast response of deeper living species to temperature fluctuations indicates that abundance of fish species can change as quick in great depths as in shallow depths, which sheds new light on fish dynamics in deep slope regions. Abundance of fish in Greenland waters can be influenced by local and external physical and biological processes. Local processes may consist of changes affecting fish growth, reproduction and survival, while changes in conditions in adjacent areas could as well affect migration or drift patterns of early life stages and thereby affect local abundance (Biro, Beckmann, & Stamps, 2010; Dahlke et al., 2018; Kuczynski, Chevalier, Laffaille, Legrand, & Grenouillet, 2017; Souza, Ilarri, Timóteo, Marques, & Martins, 2018). As local temperature is not the only mechanistic driver of these processes, we discuss the role of temperature and other pathways linked to the distribution of mode waters in the North Atlantic as guidance for future research.

## 4.1. The mechanistic role of temperature

All boreal species are expected to encounter the lower edge of their thermal affinity at a particular point in our study region (Mecklenburg et al., 2018), which thereby limits their distribution. Because distribution and abundance for many species are positively correlated through fish density dependent processes (Blanchard et al., 2005; Ralston, DeLuca, Feldman, & King, 2017; Zimmermann, Ricard, & Heino, 2018), it is expected that abundance of boreal fish in Greenland waters increases with increasing thermal habitat. Temperature can affect fish, and in turn their abundance through direct physiological responses as well as indirect through predation and food availability (Bakun, 1996; Lloret, Shulman, & Love, 2013; Pörtner & Peck, 2010).

Unlike the unequivocal effect of expansion/contraction of the thermal habitat, indirect effects through the food web are more complex and less well understood in East Greenland waters. No comprehensive information exists on the functional relationship between temperature and productivity of low-trophic level prey species. In Southwest- and West Greenland waters zooplankton abundance is higher during warm periods (Pedersen & Smidt, 2000). Because these areas act as nursery grounds for several boreal fish species, such as Atlantic cod, blue whiting, redfish (*Sebastes mentella* and *S. norvegicus*, Sebastidae) and wolffish (*Anarhichas* spp., Anarhichadidae) (Pedersen & Kanneworff, 1995; Pedersen & Rice, 2002; Post et al., 2019), it appears that survival of the early life stages could benefit from increased abundance of zooplankton species, such as the copepod *Calanus finmarchicus*, during periods of higher temperatures (Pedersen & Smidt, 2000). Higher zooplankton availability could lead to improved feeding conditions for fish species higher in the food chain. This might cause intensified feeding migrations of for example saithe, which was recaptured in Greenland waters in the early 2000s after being tagged in Iceland, indicating that such mobile species migrate to Greenland waters (ICES, 2019). On the other hand, during periods of strong SPG, when temperatures decrease, vertical mixing increases and thereby brings limiting minerals essential for phytoplankton communities, such as silicate, to the surface waters in the Irminger and Labrador Seas (Hátún et al., 2017). This can contribute to higher food availability in off-shelf regions, such as south of Iceland, where zooplankton biomass is positively correlated with the SPG (Hátún et al., 2016). As studies thereby show contradicting relationships between zooplankton, temperature and SPG regimes, it is difficult to draw conclusions about how food availability changes with temperature. Nevertheless, observations of zooplankton (including fish larvae) numbers in South and West Greenland suggest a positive correlation with temperature, which suggests that in shelf and slope regions zooplankton production is locally decoupled from the ocean basins of the Labrador and Irminger Seas. The cold and fresh East Greenland current (Figure 1) could play an important role in this context and warmer temperatures might be observed when less Arctic waters enter regions on and along the Greenland shelf.

## 4.2. The possible impact of mode waters on fish abundance

Our results suggest that temperature is the most important physical parameter regulating abundance of boreal fish in Greenland. Furthermore, because LD and RD, which are mainly affected by variability in mode waters, correlated with abundance for more species than temperature (Table 1), it appears that additional confounding parameters intrinsically related to variability in the SPG, can affect abundance. Water density correlates with temperature, salinity, current strength and oxygen content (Rhein, Steinfeldt, Kieke, Stendardo, & Yashayaev, 2017), which affect fish behaviour and physiology (Kisten, Strydom, Perissinotto, Mpinga, & Paul, 2019; Pörtner et al., 2001). Salinity and current speed, however, showed weaker correlations with abundance and hence seem to be of minor importance than temperature (Table 1). Sound information on oxygen content along the shelf was not available, but as oxygen content in the Labrador and Irminger Sea is positively linked with the SPG (Rhein et al., 2017) (the opposite direction of abundance), changes in oxygen content are unlikely a driver of abundance. The additional effect from the mode water variability, seem therefore to be taking place outside the study area. This may be through bottom up processed as explained above and/or by affecting migration patterns of the fish species.

As the Irminger current passes the western coast of Iceland, before it enters Greenland waters, eggs and larvae of haddock, Atlantic cod and capelin (*Mallotus villosus*, Osmeridae) occasionally drift from Icelandic spawning grounds to Southwest Greenland waters, which positively affects local abundance of these species (Buch, Horsted, & Hovgård, 1994; Vilhjálmsson & Fridgeirsson, 1976; Wieland & Hovgård, 2002). Because especially non-commercial and deep slope species investigated in this study are notoriously under-researched and their spawning grounds are unknown, it cannot be excluded that their abundance in Greenland waters is affected by influx events from Iceland, which might be linked to processes regulated by the SPG. Abundance estimates for blue ling, greater argentine, haddock, ling, saithe and tusk in Iceland waters, seem to follow similar temporal trends (ICES, 2018a, 2018b). This indicates that abundance of several boreal species, which we investigated in our study, is subject to similar environmental forcing in Iceland waters and as well linked to the overarching role of the subpolar gyre.

## 4.3. Projections under climate change

Prediction of fish abundance is recognized as a challenging task, as both physical and biological processes must be incorporated, and especially the latter is difficult (Payne, Hobday, Mackenzie, & Tommasi, 2019; Payne et al., 2017). The impacts of climate change will vary across regions in Greenland waters. Strongest temperature changes are expected to happen in high Arctic areas, while changes in the subpolar gyre region and the southern Labrador Sea are predicted to be smaller (IPCC, 2013, 2019; Peck & Pinnegar, 2018). The Atlantic Meridional Overturning Circulation (AMOC), is predicted to decline due to atmospheric warming and additional inflow of fresh water from ice melting, which both tend to intensify stratification and thus weaken convection (Collins et al., 2013; IPCC, 2019; Weaver et al., 2012). However, convection depth in the Labrador Sea in recent years have been some of the deepest ever observed (back to the 1930s) (Yashayaev & Loder, 2017). Thus, long-term climate projections related to the main processes in the SPG region are uncertain (IPCC, 2019). This may both be due to the relatively coarse spatial resolution in such models, and due to the complexity of the multiple oceanographic and atmospheric processes governing these waters. On the long term, the northern regions are predicted to become more suitable for boreal species as a result of increases in temperature (Fossheim et al., 2015; Kortsch et al., 2015). With this study's results of increased abundance of boreal fishes during warm periods, it can be expected that boreal fishes will increase in numbers in the future, both in shallow and deep regions. In addition, the predicted weakening of the SPG will further enhance this process. Increasing habitat suitability for boreal fish might further enhance survival of larvae drifting with ocean currents and thereby experience higher colonization from surrounding regions as recently seen in northern East Greenland (Andrews et al., 2019; Christiansen et al., 2016; Strand, Sundby, Albretsen, & Vikebø, 2017). Our results improve the foundation for prediction of boreal fish abundance in Greenland in a warming future, while accounting for the natural variability of the SPG.

## 5. Conclusion

We demonstrate that during warm periods, boreal fish species with varying life history characteristics, habitats and depth preferences, increase in abundance in shelf regions around Greenland. Both shallow and deeper living species reacted to temperature on a multiannual time scale. Abundance and local shelf-temperatures correlated negatively with water densities of mode waters in the Labrador and Irminger Seas, which represents properties of the subpolar gyre. Our findings that abundance has a lagged response to Eastern Mode Waters, suggest that trends in abundance for boreal fish species around Greenland can be predicted several years in advance.

## 6. Acknowledgements

We wish to thank the crews from Greenland and Germany that sampled and processed the many fish analysed in the present study. We thank Heino Fock for contributing German survey data. We thank Hao

Zuo of the European Centre for Medium-Range Weather Forecasts for his help with the ORAS5 data. Discussions about the significance of the auto-correlated time-series with Anna Akimova and particularly with Prof. Dudley B. Chelton are highly appreciated. We would also like to thank the Greenland Research Council and the Danish Government for funding via "Danish State funding for Arctic Research". K.M.W. received financial support from the CLIMA project, reference RER 15/0008, Ministry of Foreign Affairs Norway. H.H. is supported by the Blue-Action project which has received funding from the European Union's Horizon 2020 research and innovation programme under grant agreement No 727852. The authors have no conflict of interests. Data used in this study can be made available upon request.

# 7. References


Akaike, H. (1974). A new look at the statistical model identification. In *EEE Transactions on Automatic Control, vol. 19, no. 6* (pp. 716–723).

Andrews, A. J., Christiansen, J. S., Bhat, S., Lynghammar, A., Westgaard, J. I., Pampoulie, C., & Præbel, K. (2019). Boreal marine fauna from the Barents Sea disperse to Arctic Northeast Greenland. *Scientific Reports*, *9*(1), 1–8. https://doi.org/10.1038/s41598-019-42097-x

Bakun, A. (1996). *Patterns in the ocean: ocean processes and marine population dynamics*. (M. California Sea Grant, in cooperation with Centro de Investigaciones Biologicas del Noroeste, La Paz, Ed.).

Berg, C. W., Nielsen, A., & Kristensen, K. (2014). Evaluation of alternative age-based methods for estimating relative abundance from survey data in relation to assessment models. *Fisheries Research*, *151*, 91–99. https://doi.org/10.1016/j.fishres.2013.10.005

Biro, P. A., Beckmann, C., & Stamps, J. A. (2010). Small within-day increases in temperature affects boldness and alters personality in coral reef fish. *Proceedings of the Royal Society B: Biological Sciences*, *277*(1678), 71–77. https://doi.org/10.1098/rspb.2009.1346

Blanchard, J. L., Mills, C., Jennings, S., Fox, C. J., Rackham, B. D., Eastwood, P. D., & O'Brien, C. M. (2005). Distribution-abundance relationships for North Sea Atlantic cod (Gadus morhua): Observation versus theory. *Canadian Journal of Fisheries and Aquatic Sciences*, *62*(9), 2001–2009. https://doi.org/10.1139/f05-109

Buch, E., Horsted, S. A., & Hovgård, H. (1994). Fluctuations in the occurrence of cod in Greenland waters and their possible causes. *ICES Journal of Marine Science*, (198), 158–174.

Burnham, K. P., & Anderson, D. R. (2002). *Model selection and multitude inference: a practical information-theoretic approach* (2nd ed.). Springer.

Cheung, W. W. L., Lam, V. W. Y., Sarmiento, J. L., Kearney, K., Watson, R., & Pauly, D. (2009). Projecting global marine biodiversity impacts under climate change scenarios. *Fish and Fisheries*, *10*(3), 235–251. https://doi.org/10.1111/j.1467-2979.2008.00315.x

Christiansen, J. S., Bonsdorff, E., Byrkjedal, I., Fevolden, S., Karamushko, O. V, Lynghammar, A., … Wienerroither, R. M. (2016). Novel biodiversity baselines outpace models of fish distribution in Arctic waters. *The Science of Nature*, *103*(8), 6. https://doi.org/10.1007/s00114-016-1332-9

Christiansen, J. S., Mecklenburg, C. W., & Karamushko, O. V. (2014). Arctic marine fishes and their fisheries in light of global change. *Global Change Biology*, *20*(2), 352–359. https://doi.org/10.1111/gcb.12395

Collins, M. R., Knutti, R., Arblaster, J., Dufresne, J.-L., Fichefet, T., Friedlingstein, P., … Wehn, M. (2013). *Long-term Climate Change: Projections, Com-mitments and Irreversibility. In: Climate Change 2013: The Physical Science Basis. Contribution of Working Group I to the Fifth Assessment Report of the Intergovernmental Panel on Climate Change [Stocker, T.F.*

Collins, M., Knutti, R., Arblaster, J., Dufresne, J.-L., Fichefet, T., Friedlingstein, P., Gao, X., Gutowski, W.J., Johns, T., Krinner, G., Shongwe, M., Tebaldi, C., Weaver, A.J. and Wehner, M. (2013): *Long-term Climate Change: Projections, Com-mitments and Irreversibility. In: Climate Change 2013: The Physical Science Basis. Contribution of Working Group I to the Fifth Assessment Report of the Intergovernmental Panel on Climate Change* [Stocker, T.F., D. Qin, G.-K. Plattner, M. Tignor, S.K. Allen, J. Boschung, A. Nauels, Y. Xia, V. Bex and P.M. Midgley (eds.)]. Cambridge University Press, Cambridge, United Kingdom and New York, NY, US

Dahlke, F. T., Butzin, M., Nahrgang, J., Puvanendran, V., Mortensen, A., Pörtner, H., & Storch, D. (2018). Northern cod species face spawning habitat losses if global warming exceeds 1.5°C. *Science Advances*, *4*, 1–11. Retrieved from https://advances.sciencemag.org/content/4/11/eaas8821/tab-pdf

Drinkwater, K. F. (2006). The regime shift of the 1920s and 1930s in the North Atlantic. *Progress in Oceanography*, *68*(2–4), 134–151. https://doi.org/10.1016/j.pocean.2006.02.011

Drinkwater, K. F., & Kristiansen, T. (2018). A synthesis of the ecosystem responses to the late 20th century cold period in the northern North Atlantic. *ICES Journal of Marine Science*, *75*, 2325–2341. https://doi.org/10.1093/icesjms/fsy077

Fock, H. (2016). Update of Groundfish Survey Results for the Atlantic Cod Greenland offshore component After re-stratification of the survey 1982-2015. *ICES CM 2016/NWWG 2016 WD22*, 1–30.

Fossheim, M., Primicerio, R., Johannesen, E., Ingvaldsen, R. B., Aschan, M. M., & Dolgov, A. V. (2015). Recent warming leads to a rapid borealization of fish communities in the Arctic. *Nature Climate Change*, *5*(7), 673–677. https://doi.org/10.1038/NCLIMATE2647

Fredston-Hermann, A., Selden, R., Pinsky, M., Gaines, S. D., & Halpern, B. S. (2020). Cold range edges of marine fishes track climate change better than warm edges. *Global Change Biology*, (January), 1–15. https://doi.org/10.1111/gcb.15035

Gill, A. E., & Niller, P. P. (1973). The theory of the seasonal variability in the ocean. *Deep-Sea Research*, *20*, 141–177.

Good, S. A., Martin, M. J., & Rayner, N. A. (2013). EN4: Quality controlled ocean temperature and salinity profiles and monthly objective analyses with uncertainty estimates. *Journal of Geophysical Research: Oceans*, *118*(12), 6704–6716. https://doi.org/10.1002/2013JC009067

Gouretski, V., & Reseghetti, F. (2010). On depth and temperature biases in bathythermograph data: Development of a new correction scheme based on analysis of a global ocean database. *Deep-Sea Research Part I: Oceanographic Research Papers*, *57*(6), 812–833. https://doi.org/10.1016/j.dsr.2010.03.011

Häkkinen, S., & Rhines, P. B. (2004). Decline of Subpolar North Atlantic Circulation during the 1990s. *Science*, *304*(5670), 555–559. https://doi.org/10.1126/science.1094917

Hansen, P. M. (1949). Studies on the Biology of the Cod in Greenland Waters. *ICES*, (123), 1–82. https://doi.org/10.2307/3564720

Hastie, T., & Tibshirani, R. (1986). Generalized Additive Models. *Statistical Science*, *1*(3), 297–318.

Hastings, R. A., Rutterford, L. A., Freer, J. J., Collins, R. A., Simpson, S. D., Genner, M. J., … Simpson, S. D. (2020). Climate Change Drives Poleward Increases and Equatorward Declines in Marine Species Report Climate Change Drives Poleward Increases and Equatorward Declines in Marine Species. *Current Biology*, 1–6.

Hátún, H., & Chafik, L. (2018). On the Recent Ambiguity of the North Atlantic Subpolar Gyre Index. *Journal of Geophysical Research: Oceans*, *123*(8), 5072–5076. https://doi.org/10.1029/2018JC014101

Hátún, H., Lohmann, K., Matei, D., Jungclaus, J. H., Pacariz, S., Bersch, M., … Reid, P. C. (2016). An inflated subpolar gyre blows life toward the northeastern Atlantic. *Progress in Oceanography*, *147*, 49–66. https://doi.org/10.1016/j.pocean.2016.07.009

Hátún, H., Payne, M. R., Beaugrand, G., Reid, P. C., Sandø, A. B., Drange, H., … Bloch, D. (2009). Large bio-geographical shifts in the north-eastern Atlantic Ocean: From the subpolar gyre, via plankton, to blue whiting and pilot whales. *Progress in Oceanography*, *80*(3–4), 149–162. https://doi.org/10.1016/j.pocean.2009.03.001

Hátún, H., Somavilla, R., Rey, F., Johnson, C., & Mathis, M. (2017). The subpolar gyre regulates silicate concentrations in the North Atlantic. *Scientific Reports*, *7*(May), 1–9. https://doi.org/10.1038/s41598-017-14837-4

Hauke, J., & Kossowski, T. (2011). Comparison of values of pearson's and spearman's correlation coefficients on the same sets of data. *Quaestiones Geographicae*, *30*(2), 87–93. https://doi.org/10.2478/v10117-011-0021-1

Heino, M., Engelhard, G. H., & Godø, O. R. (2008). Migrations and hydrography determine the abundance fluctuations of blue whiting (Micromesistius poutassou) in the Barents Sea. *Fisheries Oceanography*, *17*(2), 153–163. https://doi.org/10.1111/j.1365-2419.2008.00472.x

ICES. (2018a). *Report of the Working Group on the Biology and Assessment of Deep-sea Fisheries Resources (WGDEEP), 11–18 April 2018, ICES HQ, Copenhagen, Denmark. ICES CM 2018/ACOM:14*.

ICES. (2018b). Report of the Working Group on Widely Distributed Stocks (WGWIDE), 28 August -3 September 2018, Torshavn, Faroe Islands. *ICES CM 2018/ACOM:23*, (August), 1–576.

ICES. (2019). *North Western Working Group(NWWG).ICES Scientific Reports. 1:14. 826pp. http://doi.org/10.17895/ices.pub.5298*.

IPCC. (2013). *Climate Change 2013: The Physical Science Basis. Contribution of Working Group I to the Fifth Assessment Report of the Intergovernmental Panel on Climate Change [Stocker, T.F., D. Qin, G.-K. Plattner, M. Tignor, S.K. Allen, J. Boschung, A. Nauels, Y. Xia,.*

IPCC. (2019). *Summary for Policymakers. In: IPCC Special Report on the Ocean and Cryosphere in a Changing Climate [H.-O. Pörtner, D.C. Roberts, V. Masson-Delmotte, P. Zhai, M. Tignor, E. Poloczanska, K. Mintenbeck, M. Nicolai, A. Okem, J. Petzold, B. Rama, N. Weyer (eds.)]. In press*.

Irwin, B. J., Wagner, T., Bence, J. R., Kepler, M. V., Liu, W., & Hayes, D. B. (2013). Estimating spatial and temporal components of variation for fisheries count data using negative binomial mixed models. *Transactions of the American Fisheries Society*, *142*(1), 171–183. https://doi.org/10.1080/00028487.2012.728163

Jensen, A. S., & Hansen, P. M. (1931). Investigations on the Greenland Cod. *Rapp. P.-v. Réun. Cons. Int. Explor. Mer*, *72*, 1–74.

Johnson, C., Inall, M., & Häkkinen, S. (2013). Declining nutrient concentrations in the northeast Atlantic as a result of a weakening Subpolar Gyre. *Deep-Sea Research Part I*, *82*(2013), 95–107. https://doi.org/10.1016/j.dsr.2013.08.007

Jørgensen, O. A. (2017). Survey for Greenland Halibut in NAFO Divisions 1C-1D, 2016. *Northwest Atlantic Fisheries Organization - NAFO SCR Doc. 117/021*, 1–45.

Jørgensen, O. A., Hvingel, C., & Møller, P. R. (2015). Bottom Fish Assemblages at the Shelf and Continental Slope off East. *Journal of Natural Products 2010 73 (5), 942-948 10.1021/Np100142h, 47*, 37–49. https://doi.org/10.2960/J.v47.m706

Kisten, Y., Strydom, N. A., Perissinotto, R., Mpinga, M. S., & Paul, S. (2019). Physiological responses of a juvenile marine estuarine-dependent fish (Family Sparidae) to changing salinity. *Fish Physiology and Biochemistry*, *45*(5), 1523–1531. https://doi.org/10.1007/s10695-019-00637-2

Kortsch, S., Primicerio, R., Fossheim, M., Dolgov, A. V, Aschan, M., & Kortsch, S. (2015). Climate change alters the structure of arctic marine food webs due to poleward shifts of boreal generalists. *Proc Biol Sci*, *282*, 1–9. https://doi.org/10.5061/dryad.73r6j

Kuczynski, L., Chevalier, M., Laffaille, P., Legrand, M., & Grenouillet, G. (2017). Indirect effect of temperature on fish population abundances through phenological changes. *PLoS ONE*, *12*(4), 1–13. https://doi.org/10.1371/journal.pone.0175735

Lloret, J., Shulman, G., & Love, R. M. (2013). *Condition and Health Indicators of Exploited Marine Fishes*. Chichester, England: John Wiley & Sons Ltd.

Maunder, M. N., & Punt, A. E. (2004). Standardizing catch and effort data: A review of recent approaches. *Fisheries Research*, *70*(2-3 SPEC. ISS.), 141–159. https://doi.org/10.1016/j.fishres.2004.08.002

Mecklenburg, C. W., Lynghammer, A., Johannesen, E., Byrkjedal, I., Christiansen, J. S., Dolgov, A. V, … Wienerroither, R. M. (2018). *Marine Fishes of the Arctic region*. *Conservation of Arctic Flora and Fauna* (Vol. I).

Møller, P. R., Nielsen, J. G., Knudsen, S. W., Poulsen, J. Y., Sünksen, K., & Jørgensen, O. A. (2010). *Fish fauna of Greenland waters*. *Zootaxa (2378)* (Vol. 84).

Núñez-Riboni, I., Kristinsson, K., Bernreuther, M., van Aken, H. M., Stransky, C., Cisewski, B., & Rolskiy, A. (2013). Impact of interannual changes of large scale circulation and hydrography on the spatial distribution of beaked redfish (Sebastes mentella) in the Irminger Sea. *Deep-Sea Research Part I: Oceanographic Research Papers*, *82*, 80–94. https://doi.org/10.1016/j.dsr.2013.08.003

ORAS5. (2019). Data from the Ocean ReAnalysis System 5, downloaded from: https://icdc.cen.uni-hamburg.de/daten/reanalysis-ocean/easy-init-ocean/ecmwf-oras5.html. Access: May, 2019.

Payne, M. R., Hobday, A. J., Mackenzie, B. R., & Tommasi, D. (2019). Editorial: Seasonal-to-Decadal Prediction of Marine Ecosystems: Opportunities, Approaches, and Applications. *Frontiers in Marine Science*, *6*, 1–2.

https://doi.org/10.1002/wcc.217

Payne, M. R., Hobday, A. J., MacKenzie, B., Tommasi, D., Dempsey, D. P., Fässler, S. M. M., … Villarino, E. (2017). Lessons from the First Generation of Marine Ecological Forecast Products. *Frontiers in Marine Science*, *4*(289). Retrieved from https://www.frontiersin.org/article/10.3389/fmars.2017.00289

Peck, M. A., & Pinnegar, J. (2018). Climate change impacts, vulnerabilities and adaptations: North Atlantic and Atlantic Arctic marine fisheries. In *Barange, M., Bahri, T., Beveridge, M.C.M., Cochrane, K.L., Funge-Smith, S. & Poulain, F., eds. 2018. Impacts of climate change on fisheries and aquaculture: synthesis of current knowledge, adaptation and migration option. FAO Fisheries and Agriculture Tec* (p. 628).

Pedchenko, A. P. (2005). The role of interannual environmental variations in the geographic range of spawning and feeding concentrations of redfish Sebastes mentella in the Irminger Sea. *ICES Journal of Marine Science*, *62*(7), 1501–1510. https://doi.org/10.1016/j.icesjms.2005.08.004

Pedersen, S. A., & Kanneworff, P. (1995). Fish on the West Greenland shrimp grounds, 1988–1992. *ICES Journal of Marine Science*, *52*(2), 165–182.

Pedersen, S. A., & Rice, J. C. (2002). Dynamics of fish larvae, zooplankton, and hydrographical characteristics in the West Greenland large marine ecosystem 1950-1984. *Large Marine Ecosystems*. https://doi.org/10.1016/S1570-0461(02)80057-X

Pedersen, S. A., & Smidt, E. L. B. (2000). Zooplankton distribution and abundance in west Greenland waters, 1950-1984. *Journal of Northwest Atlantic Fishery Science*, *26*, 45–102. https://doi.org/10.2960/J.v26.a4

Perry, A. L., Low, P. J., Ellis, J. R., & Reynolds, J. D. (2005). Climate Change and Distribution Shifts in Marine Fishes. *Science*, *308 (5730)*, 1912–1915.

Pörtner, H. O., Berdal, B., Blust, R., Brix, O., Colosimo, A., De Wachter, B., … Zakhartsev, M. (2001). Climate induced temperature effects on growth performance, fecundity and recruitment in marine fish: developinga hypothesis for cause and effect relationships in Atlantic cod (Gadus morhua) and common eelpout (Zoarces viviparus). *Continental Shelf Research*, *21*, 1975–1997. https://doi.org/10.1016/j.rie.2015.11.004

Pörtner, H. O., & Peck, M. A. (2010). Climate change effects on fishes and fisheries: Towards a cause-and-effect understanding. *Journal of Fish Biology*, *77*(8), 1745–1779. https://doi.org/10.1111/j.1095-8649.2010.02783.x

Post, S., Fock, H. O., & Jansen, T. (2019). Blue whiting distribution and migration in Greenland waters. *Fisheries Research*, *212*, 123–135. https://doi.org/10.1016/j.fishres.2018.12.007

Pyper, B. J., & Peterman, R. M. (1998). Comparison of methods to account for autocorrelation in correlation analyses of fish data. *Canadian Journal of Fisheries and Aquatic Sciences*, *55*, 2127–2140.

Pyper, B. J., & Peterman, R. M. (2011). Erratum : Comparison of methods to account for autocorrelation in correlation analyses of fish data. *Canadian Journal of Fisheries and Aquatic Sciences*, *55*, 2127–2140.

R Core Team. (2018). R: A language and environment for statistical computing. R Foundation for Statistical Computing, Vienna, Austria. URL https://www.R-project.org/.

Ralston, J., DeLuca, W. V., Feldman, R. E., & King, D. I. (2017). Population trends influence species ability to track climate change. *Global Change Biology*, *23*(4), 1390–1399. https://doi.org/10.1111/gcb.13478

Retzel, A. (2017). Greenland Shrimp and Fish survey results for Atlantic cod in ICES subarea 14b (East Greenland) and NAFO subarea 1F (SouthWest Greenland) in 2016. *ICES CM 2017/NWWG WD03*, 1–22.

Retzel, A. (2019). *Greenland Shrimp and Fish survey results for Atlantic cod in NAFO subareas 1A-1E (West Greenland) in 2018*. *ICES C. 2019/NWWG WD16 1-23*.

Rhein, M., Steinfeldt, R., Kieke, D., Stendardo, I., & Yashayaev, I. (2017). Ventilation variability of Labrador Sea Water and its impact on oxygen and anthropogenic carbon: A review. *Philosophical Transactions of the Royal Society A: Mathematical, Physical and Engineering Sciences*, *375*(2102). https://doi.org/10.1098/rsta.2016.0321

Riget, F., Johansen, P., Dahlgaard, H., Mosbech, A., Dietz, R., & Asmund, G. (2000). The seas around greenland. In Asmund (Ed.), *Seas at the Millennium - an Environmental Evaluation - Volume 1* (pp. 5–16). Elsevier Science Inc.

Simpson, S. D., Jennings, S., Johnson, M. P., Blanchard, J. L., Schön, P. J., Sims, D. W., & Genner, M. J. (2011). Continental shelf-wide response of a fish assemblage to rapid warming of the sea. *Current Biology*, *21*(18), 1565–1570. https://doi.org/10.1016/j.cub.2011.08.016

Souza, A. T., Ilarri, M. I., Timóteo, S., Marques, J. C., & Martins, I. (2018). Assessing the effects of temperature and salinity oscillations on a key mesopredator fish from European coastal systems. *Science of the Total Environment*, *640–641*, 1332–1345. https://doi.org/10.1016/j.scitotenv.2018.05.348

Spearman, C. (1904). The Proof and Measurement of Association between Two Things. *The American Journal of Psychology*, *15*(1), 72–101.

Speer, K., & Forget, G. (2013). Global distribution and formation of mode waters. In *International Geophysics* (2nd ed., Vol. 103, pp. 211–226). Elsevier Ltd. https://doi.org/10.1016/B978-0-12-391851-2.00009-X

Stenberg, C., Støttrup, J. G., Van Deurs, M., Berg, C. W., Dinesen, G. E., Mosegaard, H., … Leonhard, S. B. (2015). Long-term effects of an offshore wind farm in the North Sea on fish communities. *Marine Ecology Progress Series*, *528*(May), 257–265. https://doi.org/10.3354/meps11261

Strand, K. O., Sundby, S., Albretsen, J., & Vikebø, F. B. (2017). The Northeast Greenland Shelf as a Potential Habitat for the Northeast Arctic Cod. *Frontiers in Marine Science*, *4*, 1–14. https://doi.org/10.3389/fmars.2017.00304

Tåning, Å. V. (1948). On changes in the marine fauna of the North-Western Atlantic area, with special reference to Greenland. *Rapport Er Procès-Verbaux de La Conseil Permanent International Pour l'Exploration de La Mer*, *54*, 27–29.

Tweedie, M. C. K. (1984). An index which distinguishes between some important exponential families. In Statistics: Applications and New Directions. Proceedings of the Indian Statistical Institute Golden Jubilee International Conference. (Eds. J. K. Ghosh and J. Roy). *Calcutta: Indian Statistical Institute*, 579–604.

Våge, K., Pickart, R. S., Sarafanov, A., Knutsen, Ø., Mercier, H., Lherminier, P., … Bacon, S. (2011). The Irminger Gyre: Circulation, convection, and interannual variability. *Deep-Sea Research Part I: Oceanographic Research Papers*, *58*(5), 590–614. https://doi.org/10.1016/j.dsr.2011.03.001

Vilhjálmsson, H., & Fridgeirsson, E. (1976). *A review of 0-group surveys in the Iceland-East-Greenland area in the years 1970-1975. ICES C. 1975/H34.*

Weaver, A. J., Sedlá, J., Eby, M., Alexander, K., Crespin, E., Fichefet, T., … Zickfeld, K. (2012). Stability of the Atlantic meridional overturning circulation: A model intercomparison. *Geophysical Research Letters*, *39*, 1–8. https://doi.org/10.1029/2012GL053763

Wieland, K., & Hovgård, H. (2002). Distribution and drift of Atlantic cod (Gadus morhua) eggs and larvae in Greenland offshore waters. *Journal of Northwest Atlantic Fishery Science*, *22*, 61–76. https://doi.org/10.2960/j.v30.a4

Wood, S. N. (2017). *Generalized Additive Models: An Introduction with R* (2nd ed.). CRC Press. Retrieved from https://books.google.gl/books?id=OitmjwEACAAJ

Yashayaev, I., & Loder, J. W. (2017). Further intensification of deep convection in the Labrador Sea in 2016. *Geophysical Research Letters*, *44*(3), 1429–1438. https://doi.org/10.1002/2016GL071668

Zimmermann, F., Ricard, D., & Heino, M. (2018). Density regulation in Northeast Atlantic fish populations : Density dependence is stronger in recruitment than in somatic growth. *Journal of Animal Ecology*, (April 2017), 672–681. https://doi.org/10.1111/1365-2656.12800

Zuo, H., Balmaseda, M. A., Tietsche, S., Mogensen, K., & Mayer, M. (2019). The ECMWF operational ensemble reanalysis-analysis system for ocean and sea ice: A description of the system and assessment. *Ocean Science*, *15*(3), 779–808. https://doi.org/10.5194/os-15-779-2019

Zuur, A. F., Ieno, E. N., & Elphick, C. S. (2010). A protocol for data exploration to avoid common statistical problems. *Methods in Ecology and Evolution*, *1*(1), 3–14. https://doi.org/10.1111/j.2041-210x.2009.00001.x

# Tables

Table 1: Metrics of Spearman's correlations between abundance indices and temperature, salinity current speed, LD and RD. Species sorted after modelled depth distribution with shallowest occurring in the top and deepest in the bottom. Shaded cells show correlations significant at 90%, 95% and 98% confidence levels.

| | Temperature | | Salinity | | Current speed | | LD | | RD | |
|---|---|---|---|---|---|---|---|---|---|---|
| **Species** | r | p | r | p | r | p | r | p | r | p |
| Ling | 0.57 | 0.052 | 0.45 | 0.068 | -0.01 | 0.976 | -0.70 | 0.011 | -0.34 | 0.246 |
| Saithe | 0.65 | 0.003 | 0.58 | 0.013 | -0.10 | 0.680 | -0.77 | 0.001 | -0.59 | 0.013 |
| Haddock | 0.72 | 0.000 | 0.31 | 0.138 | -0.30 | 0.161 | -0.58 | 0.005 | -0.60 | 0.002 |
| Atlantic wolffish | -0.15 | 0.731 | -0.16 | 0.610 | -0.33 | 0.305 | 0.55 | 0.197 | -0.26 | 0.506 |
| Greater argentine | 0.61 | 0.153 | 0.43 | 0.155 | 0.00 | 0.998 | -0.83 | 0.033 | -0.50 | 0.222 |
| Tusk | 0.64 | 0.125 | 0.45 | 0.136 | 0.27 | 0.421 | -0.86 | 0.021 | -0.30 | 0.489 |
| Blue whiting | 0.33 | 0.031 | 0.17 | 0.338 | 0.20 | 0.253 | -0.44 | 0.003 | -0.27 | 0.084 |
| Blue ling | 0.47 | 0.050 | 0.15 | 0.518 | 0.28 | 0.228 | -0.55 | 0.025 | -0.16 | 0.523 |
| Round ray | 0.74 | 0.033 | 0.54 | 0.031 | -0.12 | 0.693 | -0.58 | 0.167 | -0.69 | 0.050 |
| Roughhead grenadier | 0.46 | 0.041 | 0.16 | 0.522 | -0.07 | 0.781 | -0.18 | 0.550 | -0.48 | 0.053 |

Table 2: Correlation metrics between abundance indices and temperature, LD and RD using three different correlation analysis; direct abundance indices, 3 year running mean of abundance and first differenced abundance. Shaded cells show correlations significant at 90%, 95% and 98% confidence levels.

| | Temperature | | | | | | LD | | | | | | RD | | | | | |
|---|---|---|---|---|---|---|---|---|---|---|---|---|---|---|---|---|---|---|
| | Default ab | | 3 yr running mean ab | | First differenced ab | | Default ab | | 3 yr running mean ab | | First differenced ab | | Default ab | | 3 yr running mean ab | | First differenced ab | |
| **Species** | r | p | r | p | r | p | r | p | r | p | r | p | r | p | r | P | r | p |
| Ling | 0.57 | 0.052 | 0.64 | 0.101 | 0.12 | 0.494 | -0.70 | 0.011 | -0.75 | 0.052 | -0.08 | 0.664 | -0.34 | 0.246 | -0.37 | 0.361 | -0.12 | 0.508 |
| Saithe | 0.65 | 0.003 | 0.67 | 0.009 | 0.18 | 0.296 | -0.77 | 0.001 | -0.79 | 0.005 | -0.10 | 0.571 | -0.59 | 0.013 | -0.59 | 0.035 | -0.18 | 0.300 |
| Haddock | 0.72 | 0.000 | 0.73 | 0.004 | -0.27 | 0.124 | -0.58 | 0.005 | -0.63 | 0.032 | 0.23 | 0.193 | -0.60 | 0.002 | -0.65 | 0.010 | 0.27 | 0.127 |
| Atlantic wolffish | -0.15 | 0.731 | -0.11 | 0.808 | -0.38 | 0.028 | 0.55 | 0.197 | 0.53 | 0.242 | 0.30 | 0.091 | -0.26 | 0.506 | -0.32 | 0.433 | 0.40 | 0.019 |
| Greater argentine | 0.61 | 0.153 | 0.64 | 0.154 | 0.13 | 0.459 | -0.83 | 0.033 | -0.85 | 0.037 | -0.03 | 0.882 | -0.50 | 0.222 | -0.53 | 0.221 | -0.39 | 0.023 |
| Tusk | 0.64 | 0.125 | 0.60 | 0.193 | 0.20 | 0.253 | -0.86 | 0.021 | -0.84 | 0.043 | -0.09 | 0.593 | -0.30 | 0.489 | -0.25 | 0.588 | -0.12 | 0.507 |
| Blue whiting | 0.33 | 0.031 | 0.37 | 0.114 | -0.11 | 0.531 | -0.44 | 0.003 | -0.29 | 0.240 | 0.05 | 0.785 | -0.27 | 0.084 | -0.23 | 0.302 | 0.02 | 0.904 |
| Blue ling | 0.47 | 0.050 | 0.50 | 0.118 | 0.12 | 0.491 | -0.55 | 0.025 | -0.65 | 0.046 | -0.02 | 0.912 | -0.16 | 0.523 | -0.12 | 0.715 | -0.13 | 0.463 |
| Round ray | 0.74 | 0.033 | 0.71 | 0.090 | 0.25 | 0.146 | -0.58 | 0.167 | -0.67 | 0.170 | 0.09 | 0.595 | -0.69 | 0.050 | -0.71 | 0.081 | -0.08 | 0.663 |
| Roughhead grenadier | 0.46 | 0.041 | 0.46 | 0.115 | 0.26 | 0.141 | -0.18 | 0.550 | -0.27 | 0.511 | 0.05 | 0.767 | -0.48 | 0.053 | -0.55 | 0.090 | -0.11 | 0.525 |

## Figure legends

Figure 1. Map of the central and Northwest Atlantic. The Subpolar Gyre is roughly outlined in black, and the principal mode water classes, EMW (Eastern Mode Water) and WMW (Western Mode Water) are illustrated with red and blue colors, repetitively. Arrows indicates directions of the currents; IC (Irminger Current), EGC (East Greenland Current) and WGC (West Greenland Current).

Figure 2. Sample distributions of bottom trawl surveys used for modelling abundance (German groundfish survey GGS, Greenland Greenland halibut survey GHL and Greenland fish and shrimp survey SF). a) Map of Greenland and trawl positions. Light grey area displays depth contours from 0 to 500 meters. Red line shows the axis following the coast used for modelling fish abundance (Section 2.2). b) Number of samples by year. c) Number of samples by depth.

Figure 3. Log abundance indices of the ten fish species (black dots) and summer temperature (avg. Jul-Sep values at 30 positions) along the coast at depth where fish densities are highest (red dots). Curves are three year running means and horizontal dashed lines the average values. Species are sorted after depth, using the depth with highest densities. Abundance indices are catch numbers at an average survey station. Log abundance is only used for display purpose. The bottom right insert maps the locations of the 30 positions.

Figure 4. Log abundance indices of the ten fish species (black) and inverse LD (blue) and RD (purple) from 1981-2017. Curves are three year running means of the values. Species sorted after depth distribution with the shallowest occurring in the top.

Figure 5. a) Plot of mean annual LD and RD (inverted) from 1981-2017. Curves are 3 year running mean values and grey bars indicate periods plotted in c). b) Map with the location of the four transects (blue lines) plotted in c). c) Average summer temperature (Jul-Sep) in three different periods at the four transects. All transect starts near the coast of Greenland and ends off shelf.

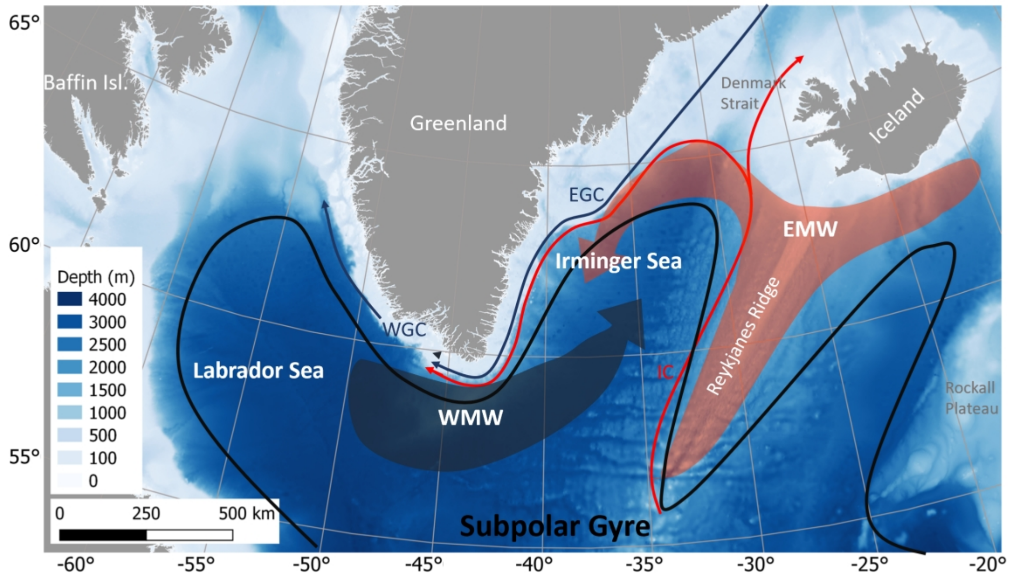


Figure 1. Map of the central and Northwest Atlantic. The Subpolar Gyre is roughly outlined in black, and the principal mode water classes, EMW (Eastern Mode Water) and WMW (Western Mode Water) are illustrated with red and blue colors, repetitively. Arrows indicates directions of the currents; IC (Irminger Current), EGC (East Greenland Current) and WGC (West Greenland Current).

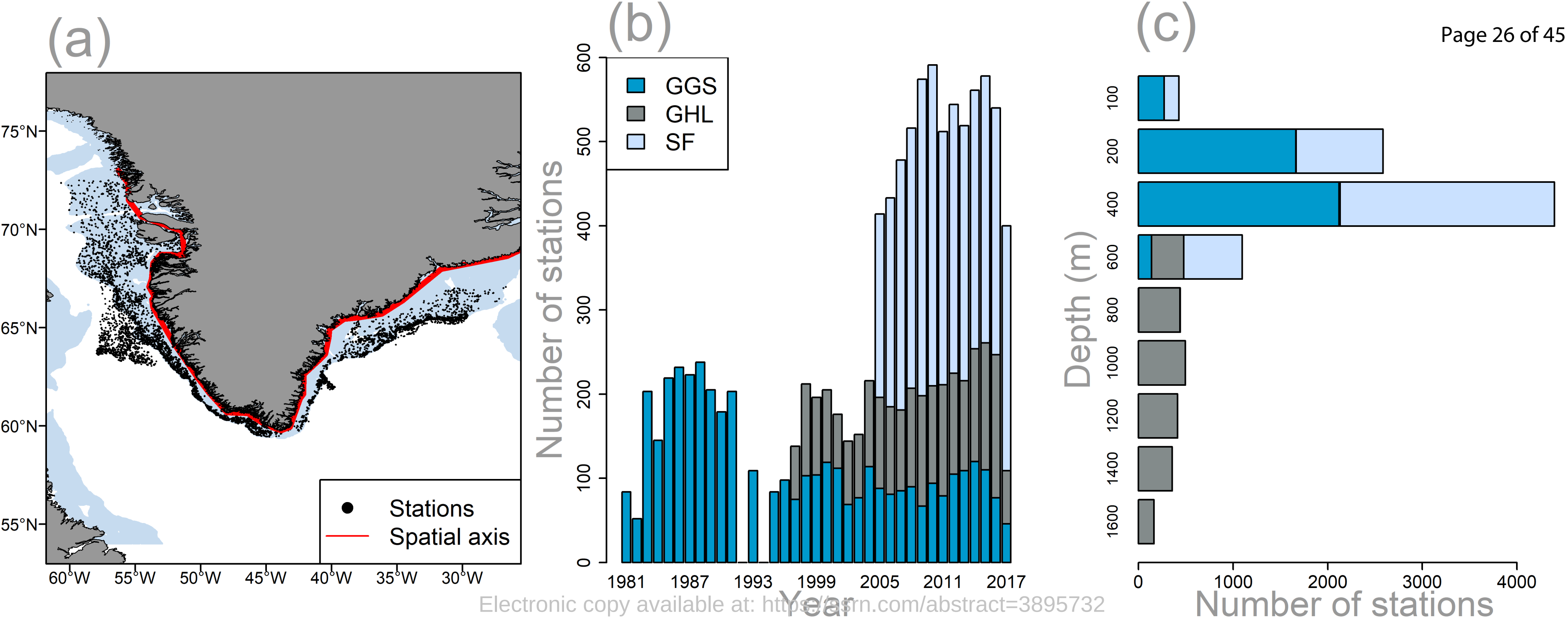
(a)
75°N
70°N
65°N
60°N
55°N
60°W
55°W
50°W
45°W
40°W
35°W
30°W
Stations
Spatial axis
(b)
GGS
GHL
SF
Number of stations
0
100
200
300
400
500
600
1981
1987
1993
1999
2005
2011
2017
Year
(c)
Depth (m)
100
200
400
600
800
1000
1200
1400
1600
0
1000
2000
3000
4000
Number of stations

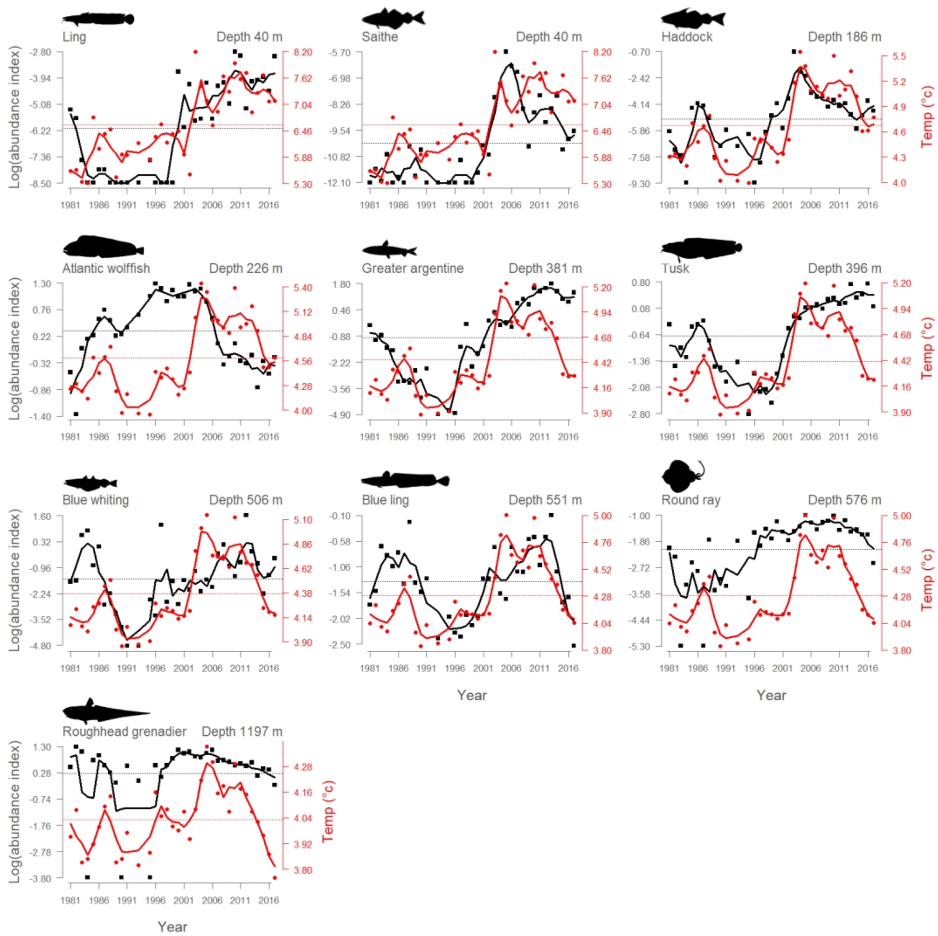


Figure 3. Log abundance indices of the ten fish species (black dots) and summer temperature (avg. Jul-Sep values at 30 positions) along the coast at depth where fish densities are highest (red dots). Curves are three year running means and horizontal dashed lines the average values. Species are sorted after depth, using the depth with highest densities. Abundance indices are catch numbers at an average survey station. Log abundance is only used for display purpose. The bottom right insert maps the locations of the 30 positions.

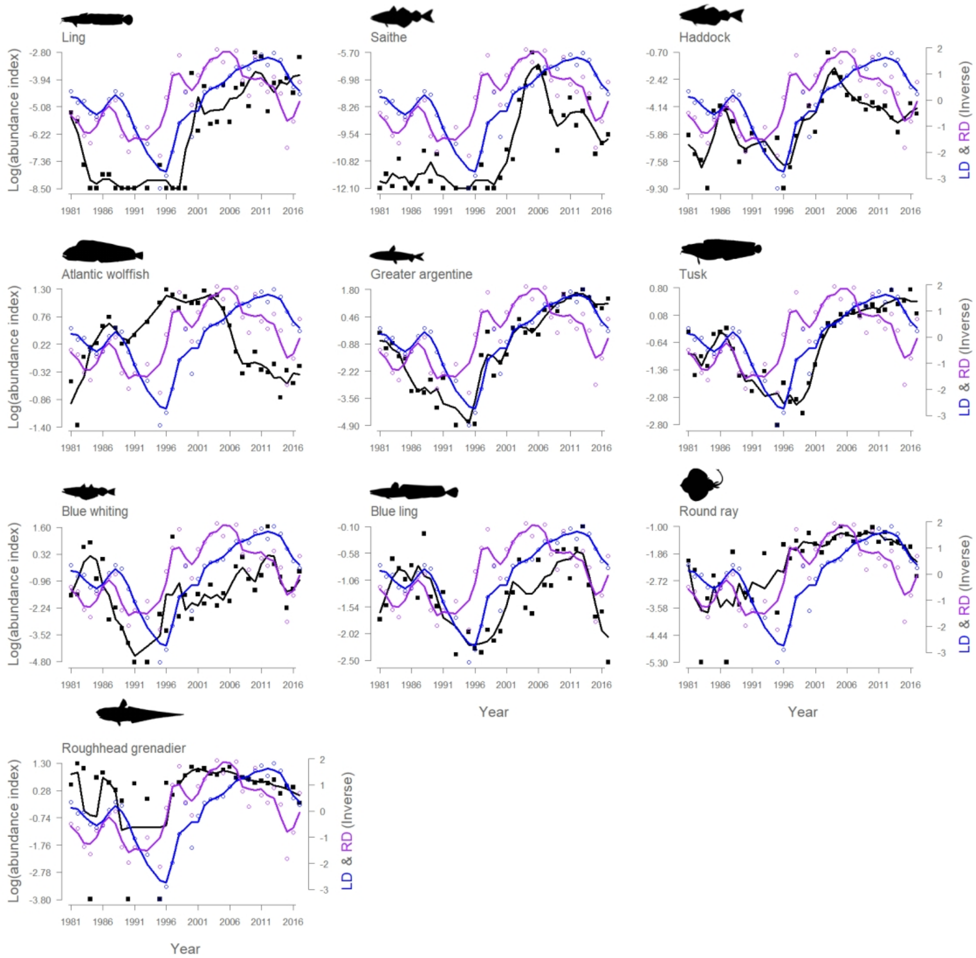


Figure 4. Log abundance indices of the ten fish species (black) and inverse LD (blue) and RD (purple) from 1981-2017. Curves are three year running means of the values. Species sorted after depth distribution with the shallowest occurring in the top.

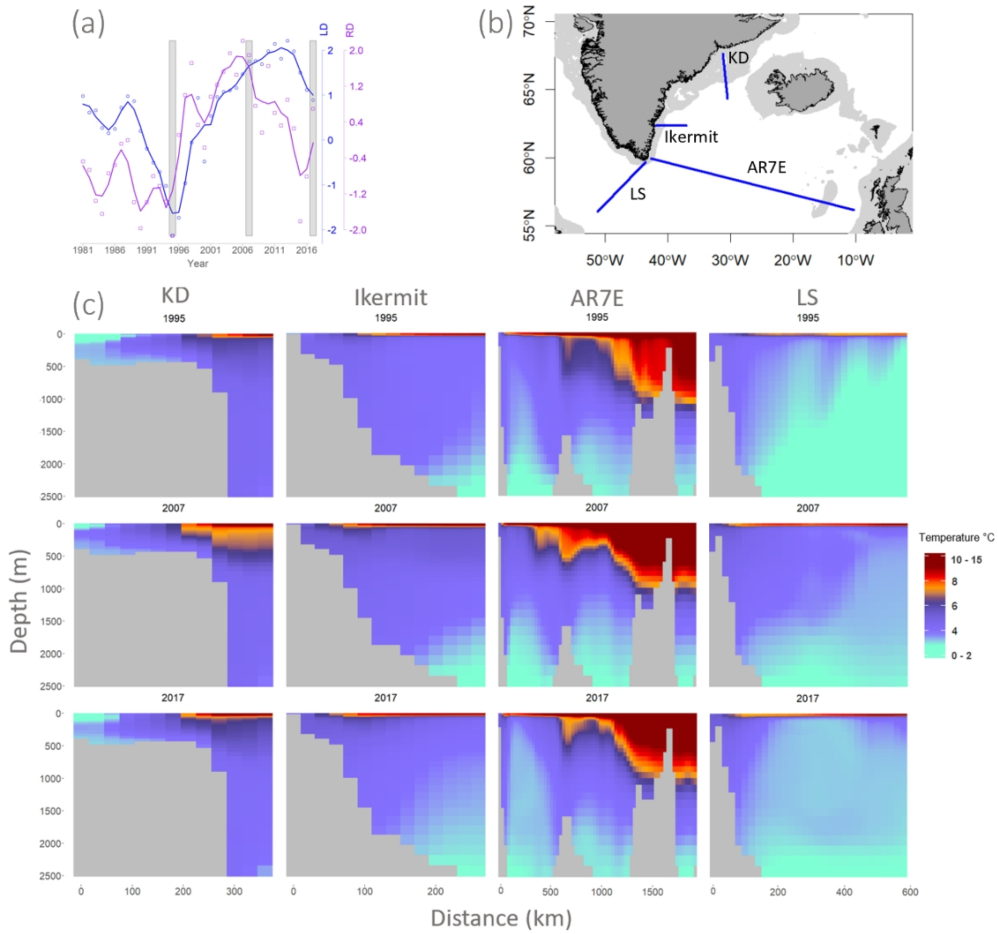


Figure 5. a) Plot of mean annual LD and RD (inverted) from 1981-2017. Curves are 3 year running mean values and grey bars indicate periods plotted in c). b) Map with the location of the four transects (blue lines) plotted in c). c) Average summer temperature (Jul-Sep) in three different periods at the four transects. All transect starts near the coast of Greenland and ends off shelf.

**Supporting Information overview**

**Supporting figures**

Fig. S1. Fish abundance on normal scale
Fig. S2. Fish abundance with standard errors
Fig. S3. Correlation values for species abundance vs. RD at different lags
Fig. S4. Horizontal correlations of temperature and water densities

**Supporting tables**

Table S1. Details of trawl surveys
Table S2. Predictor variables in the GAM
Table S3. Summary output of the chosen GAMs for every species
Table S4. Correlation metrics between abundance and temperature, LD and RD lagged

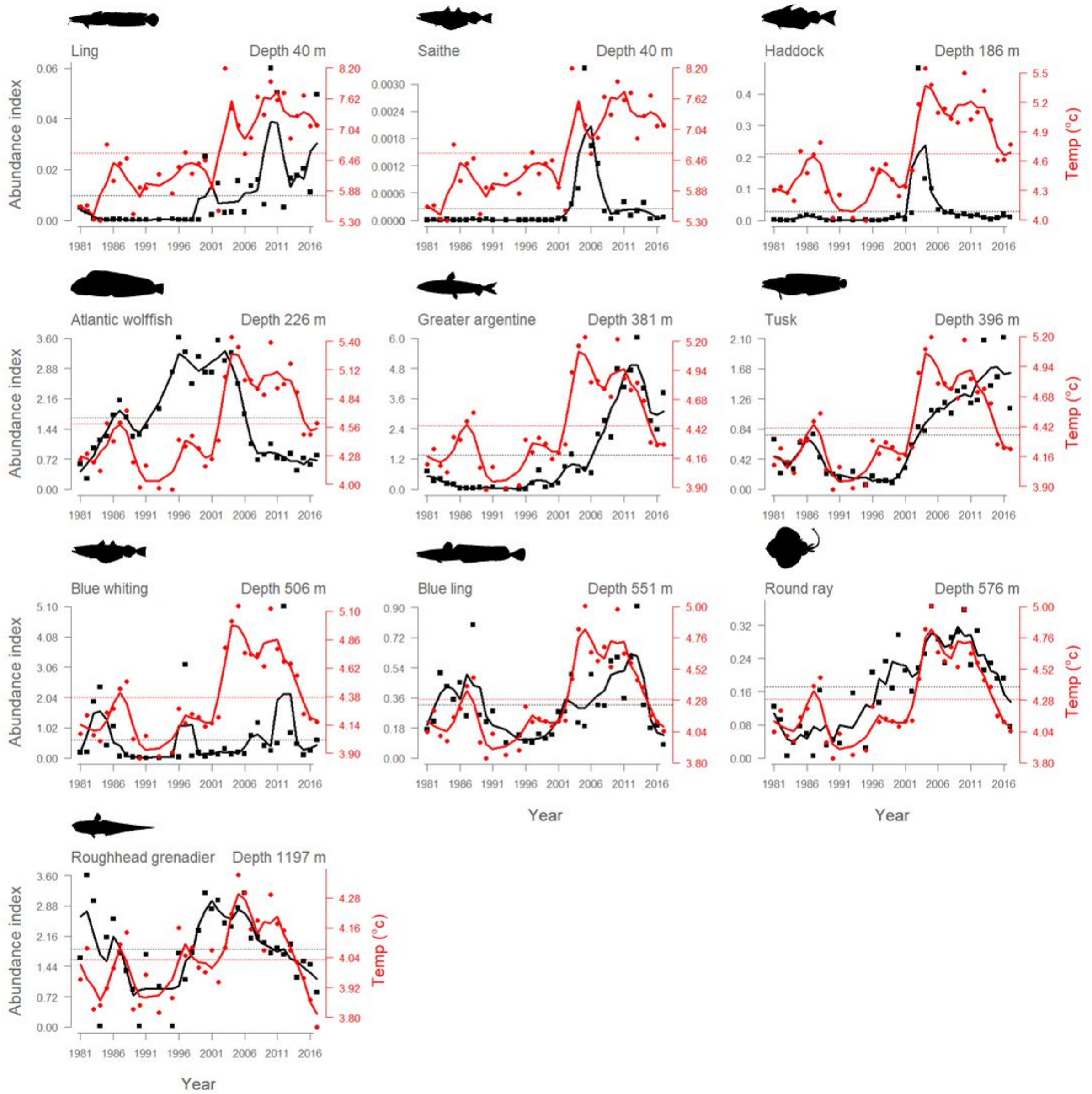


Figure S1. Abundance indices of the ten fish species (black dots) and summer temperature (avg. Jul-Sep values at 30 positions) along the coast at depth where fish densities are highest (red dots). Curves are three year running means and horizontal dashed lines the average values.

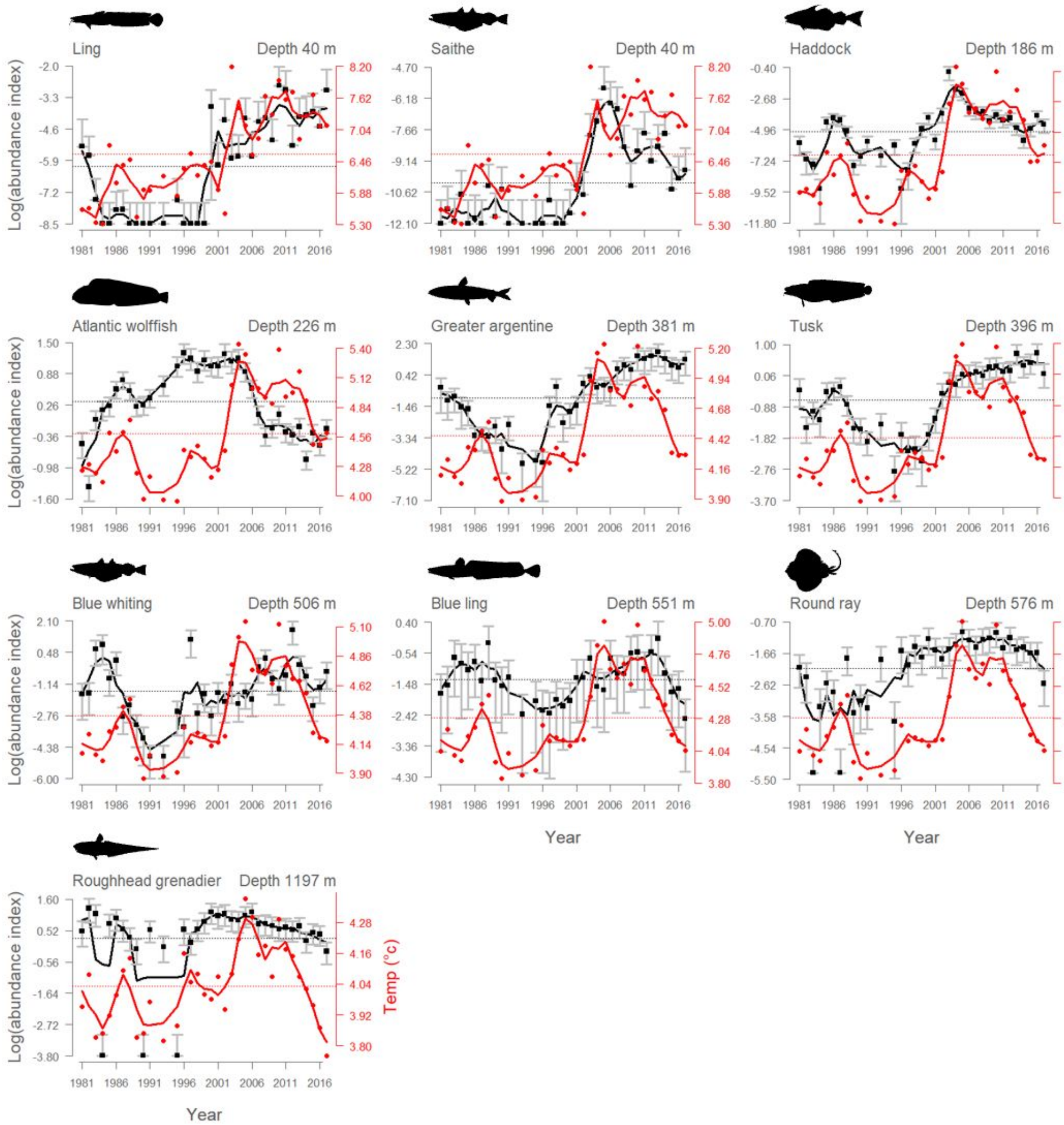


Figure S2. Log abundance indices of the ten fish species (black dots) and summer temperature (avg. Jul-Sep values at 30 positions) along the coast at depth where fish densities are highest (red dots). Curves are three year running means and horizontal dashed lines the average values. Vertical grey lines are standard errors SE. For ling, saithe and blue whiting only upper SE is shown.

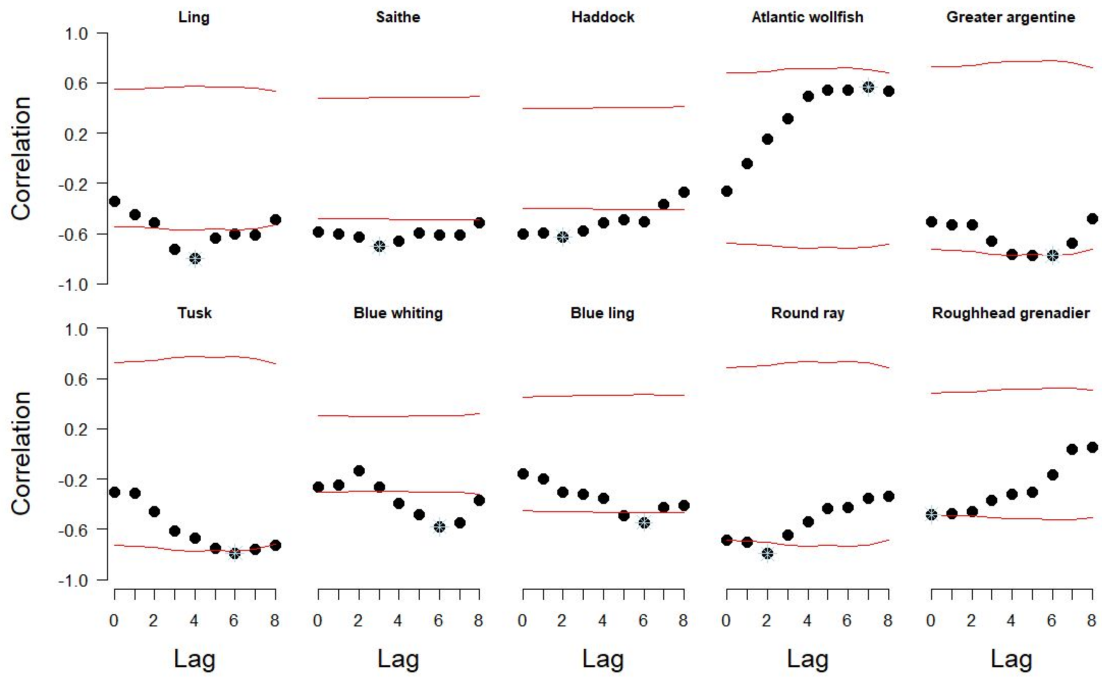


Figure S3. Correlation coefficient (r) (black) and critical correlation level (rcrit) (red) values for abundance and RD by species, at lag 0-8 years. Light blue cross indicates highest correlation.

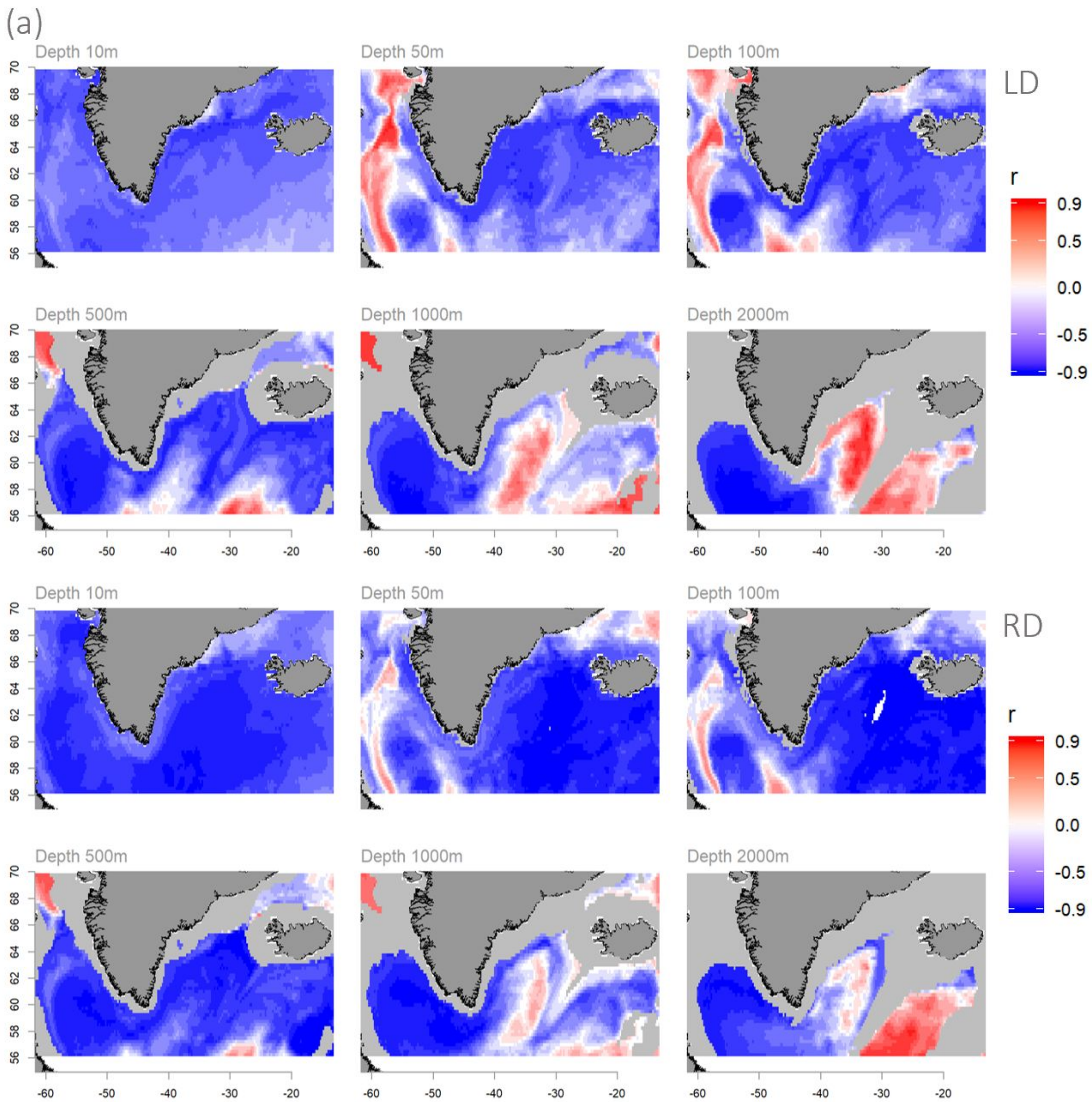

(a)
Depth 10m
Depth 50m
Depth 100m
LD
r
0.9
0.5
0.0
-0.5
-0.9
Depth 500m
Depth 1000m
Depth 2000m
-60
-50
-40
-30
-20
Depth 10m
Depth 50m
Depth 100m
RD
Depth 500m
Depth 1000m
Depth 2000m

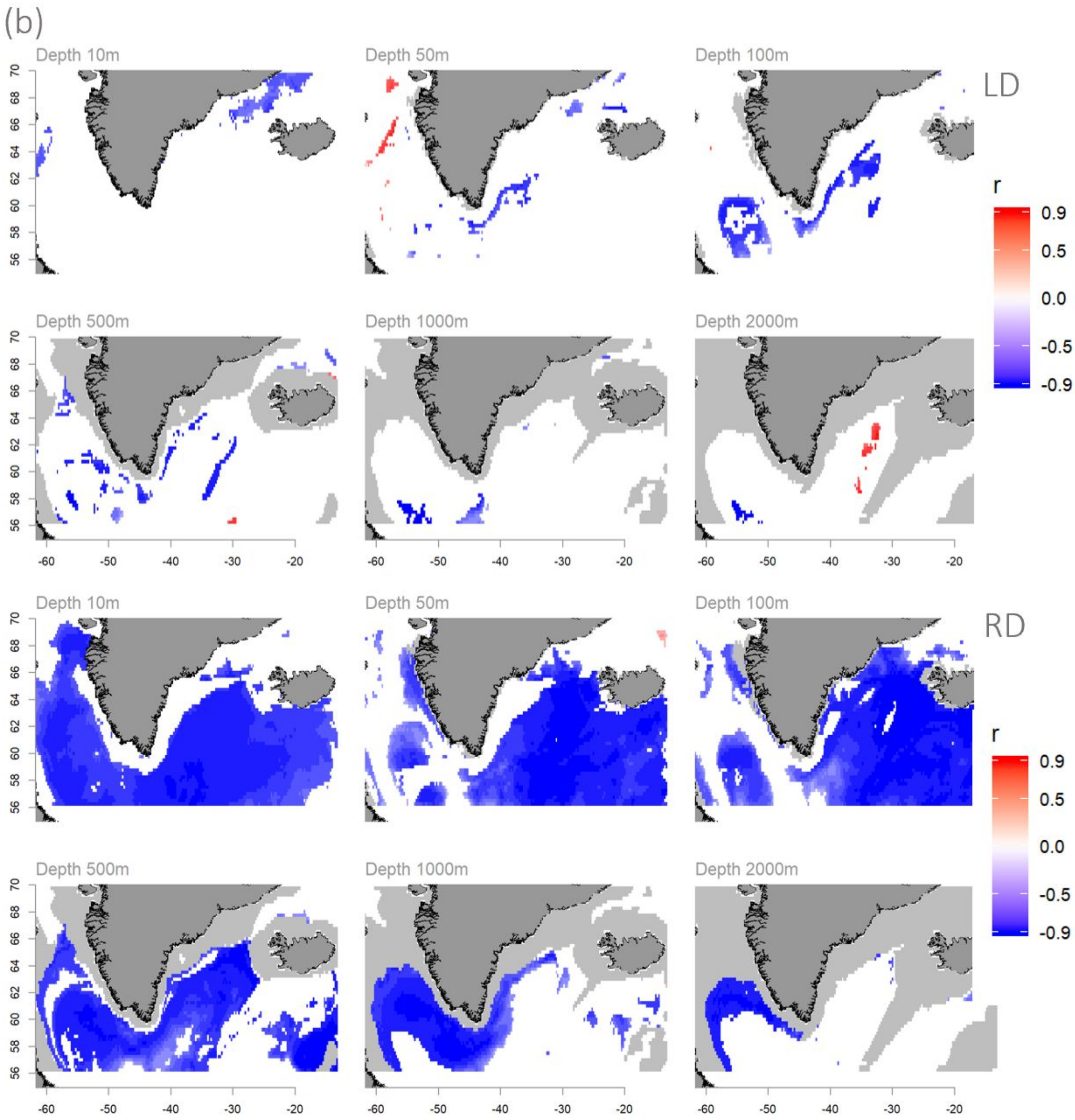


Figure S4. Horizontal correlations plots of LD and RD with temperature (Jul-Sep avg.) at six different depths, using annual 1981-2017 data. Light grey area is below ocean bottom. a) displays all correlations, while b) only correlations with $p < 0.05$.

Table S1. Details of trawl surveys used for modelling.

| Survey | Ship | Trawl gear | Haul speed (knots) | Wing spread (m) | Door spread (m) | Vertical opening (m) | From | To |
|---|---|---|---|---|---|---|---|---|
| German Greenland ground fish* (GGS) | R/V Walter Herwig II (1981-1983, 1985-1992), R/V Anton Dohrn (1984) R/V Walter Herwig III (1995-2017) | Bottom trawl | 4.5 | 25 (1981-1992) 22 (1995-2017) due to change of trawl doors | 60 | 4 | 1981 | 2017 |
| Greenland fish and shellfish** (SF) | R/V Paamiut | Cosmos trouser | 2.4 | 35 | 48 | 12 | 2005 | 2017 |
| Greenland Greenland halibut*** (GHL) | R/V Paamiut | Alfredo | 2.8 | 34 | 137 | 5.5 | 1997 | 2017 |

References: *(Fock, 2016), **(Retzel, 2017, 2019), ***(Jørgensen, 2017).

Table S2. Predictor variables in the GAM.

| Explanatory variable | Continuous vs. factor | Description |
|---|---|---|
| *Swept area* | Offset variable, Continuous | Trawled area (door spread x trawled distance) |
| *Axis* | Continuous | A location on a drawn axis following the coast, assigned by nearest distance. A value between 1 and 3179. Distance (km) from start. |
| *Depth* | Continuous | Depth of the lower trawl section |
| *Time* | Continuous | Mid time of trawling, value from 0-24 |
| *Day of Year* | Continuous | Value from 1-365 |
| *Year* | Factor | Sampling year |
| *Survey* | Factor | Survey (GGS, SF or GHL) |

Table S3. [Placed after Table S4 due to the length of it].

Table S4. Correlation metrics between abundance and temperature, LD and RD lagged.

| **Temperature vs abundance / Lag** | 0 | | 1 | | 2 | | 3 | | 4 | | 5 | | 6 | | 7 | | 8 | |
|---|---|---|---|---|---|---|---|---|---|---|---|---|---|---|---|---|---|---|
| Species | r | p | r | p | r | p | r | p | r | p | r | p | r | p | r | p | r | p |
| Ling | 0.63 | 0.021 | 0.62 | 0.022 | 0.64 | 0.015 | 0.63 | 0.017 | 0.56 | 0.034 | | | | | | | | |
| Saithe | 0.68 | 0.002 | 0.63 | 0.006 | 0.58 | 0.010 | 0.59 | 0.010 | 0.46 | 0.062 | | | | | | | | |
| Haddock | 0.69 | 0.001 | 0.53 | 0.013 | 0.45 | 0.041 | 0.34 | 0.129 | 0.24 | 0.295 | | | | | | | | |
| Atlantic wolffish | -0.29 | 0.542 | -0.53 | 0.233 | -0.71 | 0.083 | -0.77 | 0.049 | -0.82 | 0.027 | | | | | | | | |
| Greater argentine | 0.59 | 0.191 | 0.58 | 0.214 | 0.65 | 0.152 | 0.69 | 0.127 | 0.68 | 0.132 | | | | | | | | |
| Tusk | 0.60 | 0.200 | 0.63 | 0.181 | 0.71 | 0.121 | 0.73 | 0.114 | 0.72 | 0.114 | | | | | | | | |
| Blue whiting | 0.50 | 0.003 | 0.56 | 0.001 | 0.41 | 0.018 | 0.43 | 0.010 | 0.41 | 0.017 | | | | | | | | |
| Blue ling | 0.58 | 0.025 | 0.56 | 0.032 | 0.58 | 0.023 | 0.56 | 0.030 | 0.41 | 0.130 | | | | | | | | |
| Round ray | 0.73 | 0.030 | 0.61 | 0.103 | 0.59 | 0.116 | 0.41 | 0.310 | 0.36 | 0.386 | | | | | | | | |
| Roughhead grenadier | 0.53 | 0.061 | 0.38 | 0.198 | 0.21 | 0.483 | 0.20 | 0.525 | 0.11 | 0.717 | | | | | | | | |
| **LD vs abundance / Lag** | 0 | | 1 | | 2 | | 3 | | 4 | | 5 | | 6 | | 7 | | 8 | |
| Species | r | p | r | p | r | p | r | p | r | p | r | p | r | p | r | p | r | p |
| Ling | -0.70 | 0.011 | -0.77 | 0.004 | -0.68 | 0.016 | -0.66 | 0.021 | -0.55 | 0.061 | -0.45 | 0.128 | -0.44 | 0.123 | -0.32 | 0.253 | -0.24 | 0.393 |
| Saithe | -0.77 | 0.001 | -0.74 | 0.002 | -0.68 | 0.007 | -0.57 | 0.029 | -0.48 | 0.071 | -0.37 | 0.180 | -0.27 | 0.339 | -0.13 | 0.643 | -0.01 | 0.972 |
| Haddock | -0.58 | 0.005 | -0.48 | 0.025 | -0.35 | 0.114 | -0.30 | 0.172 | -0.28 | 0.212 | -0.21 | 0.345 | -0.08 | 0.726 | 0.08 | 0.729 | 0.29 | 0.190 |
| Atlantic wolffish | 0.55 | 0.197 | 0.73 | 0.060 | 0.77 | 0.039 | 0.76 | 0.044 | 0.76 | 0.041 | 0.72 | 0.056 | 0.67 | 0.078 | 0.62 | 0.098 | 0.63 | 0.077 |
| Greater argentine | -0.83 | 0.033 | -0.81 | 0.043 | -0.75 | 0.075 | -0.73 | 0.095 | -0.66 | 0.136 | -0.55 | 0.233 | -0.44 | 0.332 | -0.32 | 0.478 | -0.27 | 0.523 |
| Tusk | -0.86 | 0.021 | -0.86 | 0.024 | -0.84 | 0.028 | -0.84 | 0.031 | -0.82 | 0.035 | -0.78 | 0.051 | -0.67 | 0.100 | -0.54 | 0.186 | -0.38 | 0.355 |
| Blue whiting | -0.44 | 0.003 | -0.39 | 0.010 | -0.41 | 0.007 | -0.46 | 0.002 | -0.46 | 0.002 | -0.42 | 0.007 | -0.35 | 0.028 | -0.14 | 0.419 | -0.14 | 0.412 |
| Blue ling | -0.55 | 0.025 | -0.45 | 0.080 | -0.46 | 0.073 | -0.44 | 0.092 | -0.42 | 0.106 | -0.38 | 0.150 | -0.21 | 0.440 | -0.17 | 0.525 | -0.03 | 0.917 |
| Round ray | -0.58 | 0.167 | -0.53 | 0.222 | -0.38 | 0.400 | -0.21 | 0.645 | -0.18 | 0.701 | -0.11 | 0.811 | -0.04 | 0.925 | 0.04 | 0.920 | 0.16 | 0.687 |
| Roughhead grenadier | -0.18 | 0.550 | -0.05 | 0.863 | -0.02 | 0.953 | 0.10 | 0.738 | 0.21 | 0.489 | 0.26 | 0.376 | 0.44 | 0.120 | 0.51 | 0.063 | 0.56 | 0.037 |
| **RD vs abundance / Lag** | 0 | | 1 | | 2 | | 3 | | 4 | | 5 | | 6 | | 7 | | 8 | |
| Ling | -0.34 | 0.246 | -0.45 | 0.125 | -0.51 | 0.076 | -0.73 | 0.007 | -0.80 | 0.002 | -0.63 | 0.023 | -0.60 | 0.035 | -0.61 | 0.029 | -0.49 | 0.076 |
| Saithe | -0.59 | 0.013 | -0.60 | 0.010 | -0.63 | 0.006 | -0.70 | 0.002 | -0.66 | 0.004 | -0.60 | 0.013 | -0.61 | 0.010 | -0.61 | 0.010 | -0.52 | 0.037 |
| Haddock | -0.60 | 0.002 | -0.59 | 0.002 | -0.62 | 0.001 | -0.58 | 0.003 | -0.51 | 0.010 | -0.49 | 0.016 | -0.50 | 0.012 | -0.37 | 0.076 | -0.27 | 0.204 |
| Atlantic wolffish | -0.26 | 0.506 | -0.05 | 0.910 | 0.15 | 0.706 | 0.32 | 0.448 | 0.49 | 0.227 | 0.55 | 0.167 | 0.55 | 0.171 | 0.57 | 0.142 | 0.53 | 0.149 |
| Greater argentine | -0.50 | 0.222 | -0.53 | 0.200 | -0.53 | 0.206 | -0.66 | 0.117 | -0.77 | 0.052 | -0.77 | 0.047 | -0.78 | 0.050 | -0.67 | 0.103 | -0.48 | 0.249 |
| Tusk | -0.30 | 0.489 | -0.32 | 0.469 | -0.46 | 0.293 | -0.62 | 0.150 | -0.67 | 0.115 | -0.75 | 0.058 | -0.79 | 0.043 | -0.76 | 0.049 | -0.73 | 0.048 |
| Blue whiting | -0.27 | 0.084 | -0.25 | 0.113 | -0.14 | 0.377 | -0.27 | 0.080 | -0.39 | 0.009 | -0.49 | 0.001 | -0.58 | 0.000 | -0.55 | 0.000 | -0.37 | 0.020 |
| Blue ling | -0.16 | 0.523 | -0.20 | 0.423 | -0.30 | 0.208 | -0.32 | 0.191 | -0.35 | 0.153 | -0.50 | 0.037 | -0.54 | 0.020 | -0.43 | 0.076 | -0.41 | 0.090 |
| Round ray | -0.69 | 0.050 | -0.70 | 0.047 | -0.79 | 0.018 | -0.65 | 0.098 | -0.54 | 0.194 | -0.43 | 0.303 | -0.43 | 0.322 | -0.36 | 0.404 | -0.34 | 0.396 |
| Roughhead grenadier | -0.48 | 0.053 | -0.48 | 0.060 | -0.46 | 0.072 | -0.37 | 0.168 | -0.32 | 0.248 | -0.31 | 0.271 | -0.17 | 0.561 | 0.04 | 0.891 | 0.05 | 0.859 |

Table S3. Summary output of the chosen GAMs for every species.

```
Family: Negative Binomial(0.704)
Link function: log

Formula:
Number_Atlantic_wolffish ~ offset(log(Sweptarea_km2)) + s(Axis_km, k = 100)
+
    s(Depth_m, k = 5) + s(DayOfYear, bs = "cc", k = 5) + s(Time,
    bs = "cc", k = 5) + Year + Survey

Parametric coefficients:
             Estimate Std. Error z value Pr(>|z|)
(Intercept)   2.17266    0.20223  10.743  < 2e-16 ***
Year1982     -0.85259    0.24997  -3.411 0.000648 ***
Year1983      0.48417    0.17518   2.764 0.005712 **
Year1984      0.67237    0.18624   3.610 0.000306 ***
Year1985      0.74993    0.16969   4.419 9.90e-06 ***
Year1986      1.08181    0.19192   5.637 1.73e-08 ***
Year1987      1.26397    0.19499   6.482 9.05e-11 ***
Year1988      1.05134    0.19195   5.477 4.32e-08 ***
Year1989      0.73900    0.18855   3.919 8.88e-05 ***
Year1990      0.77428    0.18880   4.101 4.11e-05 ***
Year1991      0.90850    0.18632   4.876 1.08e-06 ***
Year1993      1.16270    0.21849   5.321 1.03e-07 ***
Year1995      1.54144    0.22631   6.811 9.69e-12 ***
Year1996      1.79884    0.21735   8.276  < 2e-16 ***
Year1997      1.69595    0.21523   7.880 3.28e-15 ***
Year1998      1.43481    0.20610   6.962 3.36e-12 ***
Year1999      1.66101    0.19829   8.377  < 2e-16 ***
Year2000      1.53823    0.21301   7.221 5.15e-13 ***
```

```
Year2001     1.53672    0.19354   7.940 2.02e-15 ***
Year2002     1.77929    0.20954   8.492  < 2e-16 ***
Year2003     1.63187    0.20020   8.151 3.60e-16 ***
Year2004     1.69230    0.19502   8.678  < 2e-16 ***
Year2005     1.43300    0.18168   7.887 3.09e-15 ***
Year2006     1.09684    0.18343   5.980 2.24e-09 ***
Year2007     0.58219    0.18224   3.195 0.001400 **
Year2008     0.15608    0.18083   0.863 0.388041
Year2009     0.31595    0.17882   1.767 0.077251 .
Year2010     0.58314    0.17572   3.319 0.000905 ***
Year2011     0.23022    0.17834   1.291 0.196736
Year2012     0.18040    0.17812   1.013 0.311165
Year2013     0.34254    0.17753   1.929 0.053676 .
Year2014    -0.30767    0.17856  -1.723 0.084881 .
Year2015     0.22054    0.17503   1.260 0.207657
Year2016    -0.02946    0.17693  -0.167 0.867759
Year2017     0.30120    0.18052   1.669 0.095212 .
SurveyGHL   -0.75339    0.16279  -4.628 3.69e-06 ***
SurveySF    -0.37942    0.12584  -3.015 0.002568 **
---
Signif. codes:  0 *** 0.001 ** 0.01 * 0.05 . 0.1   1

Approximate significance of smooth terms:
                       edf Ref.df Chi.sq p-value
s(Axis_km)          73.829 84.760 2388.4  <2e-16 ***
s(Depth_m)           3.928  3.995 1204.4  <2e-16 ***
s(DayOfYear)         2.924  3.000  311.4  <2e-16 ***
s(Time)  2.895  3.000  351.5  <2e-16 ***
---
Signif. codes:  0 *** 0.001 ** 0.01 * 0.05 . 0.1   1

R-sq.(adj) =  0.357   Deviance explained = 60.8%
-REML =  21359  Scale est. = 1         n = 10372

Family: Negative Binomial(0.214)
Link function: log

Formula:
Number_Blue_ling ~ offset(log(Sweptarea_km2)) + s(Axis_km, k = 100) +
    s(Depth_m, k = 5) + s(DayOfYear, bs = "cc", k = 5) + Year +
    Survey

Parametric coefficients:
            Estimate Std. Error z value Pr(>|z|)
(Intercept) -5.75976    7.75532  -0.743  0.45767
Year1982     0.25176    0.62879   0.400  0.68887
Year1983     1.09061    0.53779   2.028  0.04257 *
Year1984     0.91745    0.64430   1.424  0.15446
Year1985     0.71853    0.48009   1.497  0.13448
Year1986     0.97061    0.54797   1.771  0.07651 .
Year1987     0.38538    0.58650   0.657  0.51113
Year1988     1.53997    0.56421   2.729  0.00634 **
Year1989     0.40987    0.59412   0.690  0.49027
Year1990     0.23628    0.62282   0.379  0.70442
Year1991     0.49063    0.53468   0.918  0.35882
Year1993    -0.62709    0.74678  -0.840  0.40106
Year1995    -0.22556    0.70700  -0.319  0.74970
Year1996    -0.52151    0.74767  -0.698  0.48548
Year1997    -0.59388    0.70531  -0.842  0.39978
Year1998    -0.18568    0.54909  -0.338  0.73524
Year1999    -0.38388    0.54777  -0.701  0.48343
```

```
Year2000    -0.21210    0.55708  -0.381  0.70340    
Year2001     0.48080    0.51739   0.929  0.35275    
Year2002     0.48425    0.52041   0.931  0.35210    
Year2003     1.07296    0.48869   2.196  0.02812 *  
Year2004     0.20824    0.49870   0.418  0.67627    
Year2005     0.10340    0.50447   0.205  0.83759    
Year2006     1.07016    0.48754   2.195  0.02816 *  
Year2007     0.61676    0.48661   1.267  0.20499    
Year2008     0.60869    0.49181   1.238  0.21585    
Year2009     1.22202    0.47836   2.555  0.01063 *  
Year2010     1.25901    0.47995   2.623  0.00871 ** 
Year2011     0.73663    0.48038   1.533  0.12517    
Year2012     1.26319    0.47534   2.657  0.00787 ** 
Year2013     1.66967    0.47075   3.547  0.00039 ***
Year2014     0.61647    0.47925   1.286  0.19833    
Year2015     0.04696    0.48605   0.097  0.92304    
Year2016     0.14295    0.47995   0.298  0.76582    
Year2017    -0.76840    0.58423  -1.315  0.18843    
SurveyGHL    0.08409    0.34218   0.246  0.80588    
SurveySF     0.84629    0.32022   2.643  0.00822 ** 
---
Signif. codes:  0 *** 0.001 ** 0.01 * 0.05 . 0.1   1

Approximate significance of smooth terms:
                edf Ref.df Chi.sq p-value    
s(Axis_km)   43.475 51.016 478.38 < 2e-16 ***
s(Depth_m)    3.936  3.996 650.07 < 2e-16 ***
s(DayOfYear)  1.838  3.000   8.38 0.00719 ** 
---
Signif. codes:  0 *** 0.001 ** 0.01 * 0.05 . 0.1   1

R-sq.(adj) =  0.0738   Deviance explained =   70%
-REML = 3442.8  Scale est. = 1         n = 10373

Family: Negative Binomial(0.103) 
Link function: log 

Formula:
Number_Blue_whiting ~ offset(log(Sweptarea_km2)) + s(Axis_km, k = 100) + 
    s(Depth_m, k = 5) + s(DayOfYear, bs = "cc", k = 5) + Year + 
    Survey

Parametric coefficients:
              Estimate Std. Error z value Pr(>|z|)    
(Intercept) -1.917e+00  5.881e-01  -3.259 0.001119 ** 
Year1982     4.932e-02  6.934e-01   0.071 0.943295    
Year1983     2.298e+00  5.555e-01   4.137 3.52e-05 ***
Year1984     2.527e+00  6.043e-01   4.181 2.90e-05 ***
Year1985     7.916e-01  5.459e-01   1.450 0.147064    
Year1986     1.728e+00  5.833e-01   2.962 0.003056 ** 
Year1987    -1.154e+00  6.592e-01  -1.751 0.080015 .  
Year1988    -5.756e-01  6.436e-01  -0.894 0.371121    
Year1989    -1.579e+00  7.053e-01  -2.239 0.025175 *  
Year1990    -2.261e+00  7.745e-01  -2.920 0.003503 ** 
Year1991    -3.183e+00  7.080e-01  -4.496 6.94e-06 ***
Year1993    -7.483e+01  6.428e+06   0.000 0.999991    
Year1995    -8.984e-01  7.538e-01  -1.192 0.233332    
Year1996    -1.689e+00  8.196e-01  -2.061 0.039298 *  
Year1997     2.800e+00  6.039e-01   4.637 3.53e-06 ***
Year1998    -1.007e+00  6.272e-01  -1.606 0.108365    
Year1999     1.875e-02  6.029e-01   0.031 0.975193    
```

```
Year2000    -1.124e+00  6.445e-01  -1.744 0.081169 .
Year2001     5.976e-02  6.249e-01   0.096 0.923805
Year2002    -3.953e-01  6.289e-01  -0.629 0.529609
Year2003     5.119e-01  5.878e-01   0.871 0.383862
Year2004    -4.867e-01  5.921e-01  -0.822 0.411136
Year2005     9.466e-02  5.582e-01   0.170 0.865335
Year2006    -2.684e-01  5.695e-01  -0.471 0.637458
Year2007     1.378e+00  5.351e-01   2.575 0.010037 *
Year2008     1.829e+00  5.328e-01   3.432 0.000599 ***
Year2009     7.767e-01  5.326e-01   1.458 0.144716
Year2010     2.556e-01  5.385e-01   0.475 0.635022
Year2011     9.574e-01  5.322e-01   1.799 0.072028 .
Year2012     3.287e+00  5.198e-01   6.324 2.55e-10 ***
Year2013     1.496e+00  5.254e-01   2.847 0.004407 **
Year2014     8.954e-01  5.271e-01   1.699 0.089367 .
Year2015    -5.985e-01  5.367e-01  -1.115 0.264788
Year2016     3.207e-01  5.289e-01   0.606 0.544315
Year2017     1.150e+00  5.547e-01   2.073 0.038210 *
SurveyGHL    4.808e-01  3.451e-01   1.393 0.163584
SurveySF     1.355e+00  3.073e-01   4.410 1.03e-05 ***
---
Signif. codes:  0 *** 0.001 ** 0.01 * 0.05 . 0.1   1

Approximate significance of smooth terms:
                edf Ref.df Chi.sq p-value
s(Axis_km)   47.018  56.78 1083.5 < 2e-16 ***
s(Depth_m)    3.893   3.99  851.9 < 2e-16 ***
s(DayOfYear)  1.797   3.00   10.4 0.00183 **
---
Signif. codes:  0 *** 0.001 ** 0.01 * 0.05 . 0.1   1

R-sq.(adj) =  -0.0305   Deviance explained = 72.1%
-REML = 5904.6  Scale est. = 1         n = 10373

Family: Negative Binomial(0.148)
Link function: log

Formula:
Number_Greater_argentine ~ offset(log(Sweptarea_km2)) + s(Axis_km, k = 100)
+
    s(Depth_m, k = 5) + s(DayOfYear, bs = "cc", k = 5) + Year +
    Survey

Parametric coefficients:
            Estimate Std. Error z value Pr(>|z|)
(Intercept) -5.43857    7.26997  -0.748 0.454408
Year1982    -0.75924    0.63087  -1.203 0.228787
Year1983    -0.50951    0.53323  -0.956 0.339309
Year1984    -1.15297    0.61282  -1.881 0.059914 .
Year1985    -1.27429    0.50703  -2.513 0.011962 *
Year1986    -2.87780    0.58673  -4.905 9.35e-07 ***
Year1987    -2.84257    0.60813  -4.674 2.95e-06 ***
Year1988    -2.94769    0.60862  -4.843 1.28e-06 ***
Year1989    -2.31390    0.59130  -3.913 9.11e-05 ***
Year1990    -3.69722    0.72205  -5.120 3.05e-07 ***
Year1991    -2.22092    0.56511  -3.930 8.49e-05 ***
Year1993    -4.55022    0.79626  -5.714 1.10e-08 ***
Year1995    -4.36030    0.78412  -5.561 2.69e-08 ***
Year1996    -4.49428    0.87687  -5.125 2.97e-07 ***
Year1997    -1.09981    0.62162  -1.769 0.076850 .
Year1998     0.05555    0.53147   0.105 0.916757
```

```
Year1999    -2.11914    0.57698  -3.673 0.000240 ***
Year2000    -1.44888    0.57882  -2.503 0.012309 *
Year2001    -1.07336    0.56452  -1.901 0.057252 .
Year2002     0.23033    0.52741   0.437 0.662310
Year2003     0.66589    0.50895   1.308 0.190747
Year2004     0.01266    0.50690   0.025 0.980081
Year2005     0.13489    0.48675   0.277 0.781683
Year2006    -0.09113    0.49194  -0.185 0.853034
Year2007     1.12358    0.47592   2.361 0.018231 *
Year2008     1.33996    0.47661   2.811 0.004932 **
Year2009     1.06556    0.47381   2.249 0.024516 *
Year2010     1.90233    0.46804   4.064 4.81e-05 ***
Year2011     1.74003    0.46957   3.706 0.000211 ***
Year2012     1.89255    0.47003   4.026 5.66e-05 ***
Year2013     2.13643    0.46919   4.553 5.28e-06 ***
Year2014     1.72935    0.46655   3.707 0.000210 ***
Year2015     1.33745    0.46658   2.866 0.004151 **
Year2016     1.20122    0.46632   2.576 0.009996 **
Year2017     1.68282    0.48017   3.505 0.000457 ***
SurveyGHL   -1.56198    0.32921  -4.745 2.09e-06 ***
SurveySF    -1.64399    0.30530  -5.385 7.25e-08 ***
---
Signif. codes:  0 *** 0.001 ** 0.01 * 0.05 . 0.1   1

Approximate significance of smooth terms:
                edf Ref.df Chi.sq p-value
s(Axis_km)    58.181 66.387 1302.0  <2e-16 ***
s(Depth_m)     3.948  3.997  767.2  <2e-16 ***
s(DayOfYear)  2.920  3.000  169.8  <2e-16 ***
---
Signif. codes:  0 *** 0.001 ** 0.01 * 0.05 . 0.1   1

R-sq.(adj) =  -0.0399   Deviance explained = 68.6%
-REML = 7465.4  Scale est. = 1         n = 10371

Family: Negative Binomial(0.208)
Link function: log

Formula:
Number_Haddock ~ offset(log(Sweptarea_km2)) + s(Axis_km, k = 100) +
    s(Depth_m, k = 5) + s(DayOfYear, bs = "cc", k = 5) + Year +
    Survey

Parametric coefficients:
              Estimate Std. Error z value Pr(>|z|)
(Intercept) -1.743e+02  1.527e+01 -11.419  < 2e-16 ***
Year1982    -1.213e+00  7.131e-01  -1.701 0.088933 .
Year1983    -1.588e+00  5.277e-01  -3.008 0.002626 **
Year1984    -3.350e+00  9.273e-01  -3.612 0.000303 ***
Year1985     1.527e+00  4.151e-01   3.679 0.000234 ***
Year1986     1.821e+00  4.821e-01   3.777 0.000158 ***
Year1987     1.680e+00  4.917e-01   3.417 0.000633 ***
Year1988     8.599e-01  4.914e-01   1.750 0.080109 .
Year1989    -1.691e+00  5.534e-01  -3.057 0.002239 **
Year1990    -9.763e-01  5.321e-01  -1.835 0.066529 .
Year1991     9.689e-02  4.859e-01   0.199 0.841960
Year1993    -9.672e-01  6.167e-01  -1.568 0.116812
Year1995    -1.874e-01  5.999e-01  -0.312 0.754719
Year1996    -8.882e+01  6.779e+06   0.000 0.999990
Year1997    -2.040e+00  7.749e-01  -2.633 0.008472 **
Year1998    -5.422e-02  5.557e-01  -0.098 0.922268
```

```
Year1999     1.024e+00  5.010e-01   2.045 0.040901 *
Year2000     1.834e+00  5.322e-01   3.447 0.000567 ***
Year2001     2.028e-01  5.062e-01   0.401 0.688700
Year2002     2.148e+00  4.953e-01   4.336 1.45e-05 ***
Year2003     5.187e+00  4.548e-01  11.405  < 2e-16 ***
Year2004     3.893e+00  4.638e-01   8.393  < 2e-16 ***
Year2005     3.621e+00  4.487e-01   8.069 7.09e-16 ***
Year2006     2.517e+00  4.660e-01   5.400 6.66e-08 ***
Year2007     2.260e+00  4.563e-01   4.952 7.35e-07 ***
Year2008     2.295e+00  4.471e-01   5.132 2.87e-07 ***
Year2009     1.600e+00  4.499e-01   3.557 0.000375 ***
Year2010     2.036e+00  4.422e-01   4.605 4.13e-06 ***
Year2011     1.654e+00  4.454e-01   3.713 0.000205 ***
Year2012     1.827e+00  4.453e-01   4.103 4.09e-05 ***
Year2013     1.097e+00  4.502e-01   2.436 0.014859 *
Year2014     1.728e-01  4.604e-01   0.375 0.707353
Year2015     1.038e+00  4.410e-01   2.354 0.018570 *
Year2016     1.990e+00  4.290e-01   4.639 3.51e-06 ***
Year2017     1.344e+00  4.559e-01   2.947 0.003206 **
SurveyGHL   -2.088e+00  5.472e-01  -3.815 0.000136 ***
SurveySF     2.374e-01  2.869e-01   0.827 0.408125
---
Signif. codes:  0 *** 0.001 ** 0.01 * 0.05 . 0.1   1

Approximate significance of smooth terms:
                edf Ref.df Chi.sq p-value
s(Axis_km)   51.421 61.357 782.62 < 2e-16 ***
s(Depth_m)    3.981  3.999 627.06 < 2e-16 ***
s(DayOfYear)  2.558  3.000  15.32 0.00055 ***
---
Signif. codes:  0 *** 0.001 ** 0.01 * 0.05 . 0.1   1

R-sq.(adj) =  -1.57   Deviance explained =   74%
-REML = 5716.5  Scale est. = 1         n = 10373

Family: Negative Binomial(0.088)
Link function: log

Formula:
Number_Ling ~ offset(log(Sweptarea_km2)) + s(Axis_km, k = 100) +
    s(Depth_m, k = 5) + s(DayOfYear, bs = "cc", k = 5) + s(Time,
    bs = "cc", k = 5) + Year + Survey

Parametric coefficients:
              Estimate Std. Error z value Pr(>|z|)
(Intercept) -4.384e+00  2.154e+00  -2.035  0.04182 *
Year1982    -3.738e-01  1.711e+00  -0.218  0.82706
Year1983    -2.188e+00  1.895e+00  -1.155  0.24823
Year1984    -5.580e+01  5.573e+06   0.000  0.99999
Year1985    -5.696e+01  4.535e+06   0.000  0.99999
Year1986    -2.599e+00  1.908e+00  -1.363  0.17298
Year1987    -2.595e+00  1.981e+00  -1.310  0.19026
Year1988    -3.169e+00  2.062e+00  -1.537  0.12438
Year1989    -5.738e+01  4.687e+06   0.000  0.99999
Year1990    -5.670e+01  5.016e+06   0.000  0.99999
Year1991    -5.747e+01  4.710e+06   0.000  0.99999
Year1993    -5.801e+01  6.428e+06   0.000  0.99999
Year1995    -2.196e+00  2.046e+00  -1.073  0.28327
Year1996    -5.746e+01  6.779e+06   0.000  0.99999
Year1997    -5.209e+01  5.713e+06   0.000  0.99999
Year1998    -5.330e+01  4.609e+06   0.000  0.99999
```

```
Year1999    -5.313e+01  4.793e+06   0.000  0.99999
Year2000     1.636e+00  1.626e+00   1.006  0.31441
Year2001    -7.729e-01  1.701e+00  -0.454  0.64952
Year2002     1.090e+00  1.476e+00   0.739  0.46002
Year2003    -4.822e-01  1.693e+00  -0.285  0.77577
Year2004    -4.007e-01  1.594e+00  -0.251  0.80154
Year2005     1.153e+00  1.446e+00   0.797  0.42520
Year2006    -4.010e-01  1.700e+00  -0.236  0.81354
Year2007     1.018e+00  1.469e+00   0.693  0.48831
Year2008     1.174e+00  1.496e+00   0.785  0.43237
Year2009     2.517e-01  1.577e+00   0.160  0.87321
Year2010     2.500e+00  1.433e+00   1.744  0.08112 .
Year2011     2.328e+00  1.415e+00   1.645  0.09992 .
Year2012     4.121e-02  1.546e+00   0.027  0.97873
Year2013     1.219e+00  1.460e+00   0.835  0.40395
Year2014     1.280e+00  1.443e+00   0.887  0.37514
Year2015     1.421e+00  1.439e+00   0.988  0.32330
Year2016     8.138e-01  1.433e+00   0.568  0.57003
Year2017     2.311e+00  1.394e+00   1.658  0.09742 .
SurveyGHL   -2.989e+00  1.131e+00  -2.644  0.00819 **
SurveySF    -3.295e+00  1.043e+00  -3.160  0.00158 **
---
Signif. codes:  0 *** 0.001 ** 0.01 * 0.05 . 0.1   1

Approximate significance of smooth terms:
                          edf Ref.df Chi.sq  p-value
s(Axis_km)          6.384e+00  8.019 91.352 2.68e-16 ***
s(Depth_m)          2.757e+00  2.986  5.961   0.0984 .
s(DayOfYear)        1.811e+00  3.000  6.477   0.0212 *
s(Time) 5.313e-05  3.000  0.000   0.5189
---
Signif. codes:  0 *** 0.001 ** 0.01 * 0.05 . 0.1   1

R-sq.(adj) =  0.0489   Deviance explained = 67.1%
-REML = 369.36  Scale est. = 1         n = 10373

Family: Negative Binomial(0.941)
Link function: log

Formula:
Number_Roughhead_grenadier ~ offset(log(Sweptarea_km2)) + s(Axis_km, k =
100) +
    s(Depth_m, k = 5) + s(DayOfYear, bs = "cc", k = 5) + Year +
    Survey

Parametric coefficients:
              Estimate Std. Error z value Pr(>|z|)
(Intercept) -8.710e-02  2.669e-01  -0.326 0.744159
Year1982     7.884e-01  3.101e-01   2.543 0.011003 *
Year1983     6.022e-01  2.839e-01   2.121 0.033894 *
Year1984    -5.623e+01  5.573e+06   0.000 0.999992
Year1985     2.620e-01  2.646e-01   0.990 0.322068
Year1986     4.487e-01  2.760e-01   1.626 0.103955
Year1987     6.913e-02  2.905e-01   0.238 0.811890
Year1988    -2.074e-01  3.049e-01  -0.680 0.496451
Year1989    -6.117e-01  3.412e-01  -1.793 0.072974 .
Year1990    -5.704e+01  5.016e+06   0.000 0.999991
Year1991     4.413e-02  2.782e-01   0.159 0.873937
Year1993    -5.310e-01  3.610e-01  -1.471 0.141355
Year1995    -4.282e+00  1.048e+00  -4.088 4.36e-05 ***
Year1996     6.412e-02  3.551e-01   0.181 0.856719
```

```
Year1997    -3.806e-01  2.633e-01  -1.446 0.148268
Year1998     7.688e-02  2.513e-01   0.306 0.759635
Year1999     3.345e-01  2.530e-01   1.322 0.186088
Year2000     6.626e-01  2.544e-01   2.605 0.009194 **
Year2001     5.353e-01  2.417e-01   2.215 0.026759 *
Year2002     6.080e-01  2.546e-01   2.388 0.016942 *
Year2003     4.065e-01  2.515e-01   1.616 0.106047
Year2004     3.732e-01  2.394e-01   1.559 0.118945
Year2005     5.479e-01  2.493e-01   2.198 0.027943 *
Year2006     6.640e-01  2.423e-01   2.740 0.006137 **
Year2007     2.485e-01  2.491e-01   0.998 0.318399
Year2008     2.646e-01  2.499e-01   1.059 0.289692
Year2009     1.971e-01  2.495e-01   0.790 0.429566
Year2010     6.925e-02  2.510e-01   0.276 0.782666
Year2011     1.366e-01  2.506e-01   0.545 0.585868
Year2012     4.854e-02  2.510e-01   0.193 0.846623
Year2013     1.783e-01  2.519e-01   0.708 0.478983
Year2014    -3.306e-01  2.520e-01  -1.312 0.189427
Year2015    -4.943e-02  2.512e-01  -0.197 0.843995
Year2016    -1.017e-01  2.500e-01  -0.407 0.684306
Year2017    -6.905e-01  2.546e-01  -2.712 0.006683 **
SurveyGHL   -6.200e-01  1.436e-01  -4.317 1.58e-05 ***
SurveySF    -5.056e-01  1.452e-01  -3.482 0.000498 ***
---
Signif. codes:  0 *** 0.001 ** 0.01 * 0.05 . 0.1   1

Approximate significance of smooth terms:
                edf Ref.df  Chi.sq p-value
s(Axis_km)   55.973  65.47 1826.46  <2e-16 ***
s(Depth_m)    3.991   4.00 1656.43  <2e-16 ***
s(DayOfYear)  2.345   3.00   71.97  <2e-16 ***
---
Signif. codes:  0 *** 0.001 ** 0.01 * 0.05 . 0.1   1

R-sq.(adj) =  0.371   Deviance explained = 83.8%
-REML =  11070  Scale est. = 1         n = 10373

Family: Negative Binomial(0.476)
Link function: log

Formula:
Number_Round_ray ~ offset(log(Sweptarea_km2)) + s(Axis_km, k = 100) +
    s(Depth_m, k = 5) + Year + Survey

Parametric coefficients:
              Estimate Std. Error z value Pr(>|z|)
(Intercept) -1.115e+00  3.457e-01  -3.226  0.00126 **
Year1982    -2.894e-01  5.331e-01  -0.543  0.58722
Year1983    -4.800e+01  4.710e+06   0.000  0.99999
Year1984    -1.199e+00  7.347e-01  -1.632  0.10274
Year1985    -4.750e-01  4.266e-01  -1.113  0.26550
Year1986    -7.531e-01  4.307e-01  -1.749  0.08033 .
Year1987    -3.210e+00  1.065e+00  -3.013  0.00258 **
Year1988     2.765e-01  3.975e-01   0.696  0.48668
Year1989    -1.383e+00  6.106e-01  -2.265  0.02351 *
Year1990    -1.018e+00  6.298e-01  -1.617  0.10595
Year1991    -1.241e+00  4.713e-01  -2.633  0.00846 **
Year1993     2.354e-01  4.742e-01   0.496  0.61961
Year1995    -1.644e+00  8.211e-01  -2.002  0.04531 *
Year1996     5.126e-01  4.960e-01   1.033  0.30146
Year1997     7.520e-02  4.749e-01   0.158  0.87418
```

```
Year1998      6.317e-01  3.917e-01   1.613  0.10683
Year1999      3.089e-01  4.100e-01   0.753  0.45126
Year2000      8.744e-01  3.842e-01   2.276  0.02285 *
Year2001      5.337e-01  4.088e-01   1.305  0.19176
Year2002      2.588e-01  4.386e-01   0.590  0.55505
Year2003      5.599e-01  4.050e-01   1.382  0.16690
Year2004      7.050e-01  3.861e-01   1.826  0.06785 .
Year2005      1.084e+00  3.714e-01   2.917  0.00353 **
Year2006      8.355e-01  3.825e-01   2.184  0.02896 *
Year2007      6.142e-01  3.868e-01   1.588  0.11231
Year2008      8.497e-01  3.770e-01   2.254  0.02420 *
Year2009      8.971e-01  3.703e-01   2.423  0.01540 *
Year2010      1.058e+00  3.644e-01   2.904  0.00368 **
Year2011      5.939e-01  3.751e-01   1.583  0.11339
Year2012      9.066e-01  3.671e-01   2.469  0.01353 *
Year2013      5.360e-01  3.755e-01   1.428  0.15341
Year2014      6.114e-01  3.701e-01   1.652  0.09854 .
Year2015      4.386e-01  3.716e-01   1.180  0.23789
Year2016      4.424e-01  3.724e-01   1.188  0.23481
Year2017     -4.896e-01  4.963e-01  -0.986  0.32396
SurveyGHL    -9.685e-01  1.898e-01  -5.104 3.33e-07 ***
SurveySF     -2.052e-01  1.399e-01  -1.466  0.14260
---
Signif. codes:  0 *** 0.001 ** 0.01 * 0.05 . 0.1   1

Approximate significance of smooth terms:
              edf Ref.df Chi.sq p-value
s(Axis_km) 30.075 36.792  351.3  <2e-16 ***
s(Depth_m)  3.895  3.992  295.7  <2e-16 ***
---
Signif. codes:  0 *** 0.001 ** 0.01 * 0.05 . 0.1   1

R-sq.(adj) =  0.178   Deviance explained = 46.3%
-REML = 2762.6  Scale est. = 1         n = 10373

Family: Negative Binomial(0.164)
Link function: log

Formula:
Number_Saithe ~ offset(log(Sweptarea_km2)) + s(Axis_km, k = 100) +
    s(Depth_m, k = 5) + Year + Survey

Parametric coefficients:
              Estimate Std. Error z value Pr(>|z|)
(Intercept) -8.232e+01  7.322e+06   0.000   1.0000
Year1982     6.604e+01  7.322e+06   0.000   1.0000
Year1983     6.545e+01  7.322e+06   0.000   1.0000
Year1984     6.674e+01  7.322e+06   0.000   1.0000
Year1985     9.210e-01  8.613e+06   0.000   1.0000
Year1986     6.563e+01  7.322e+06   0.000   1.0000
Year1987     6.536e+01  7.322e+06   0.000   1.0000
Year1988     6.714e+01  7.322e+06   0.000   1.0000
Year1989     6.568e+01  7.322e+06   0.000   1.0000
Year1990     6.697e+01  7.322e+06   0.000   1.0000
Year1991     2.077e+00  8.706e+06   0.000   1.0000
Year1993     2.010e+00  9.743e+06   0.000   1.0000
Year1995    -8.263e-01  1.036e+07   0.000   1.0000
Year1996     1.068e+00  9.978e+06   0.000   1.0000
Year1997     6.647e+01  7.322e+06   0.000   1.0000
Year1998     3.771e+00  8.652e+06   0.000   1.0000
Year1999     3.416e+00  8.752e+06   0.000   1.0000
```

```
Year2000     6.584e+01  7.322e+06   0.000   1.0000
Year2001     6.718e+01  7.322e+06   0.000   1.0000
Year2002     6.672e+01  7.322e+06   0.000   1.0000
Year2003     6.954e+01  7.322e+06   0.000   1.0000
Year2004     7.020e+01  7.322e+06   0.000   1.0000
Year2005     7.177e+01  7.322e+06   0.000   1.0000
Year2006     7.106e+01  7.322e+06   0.000   1.0000
Year2007     7.079e+01  7.322e+06   0.000   1.0000
Year2008     6.898e+01  7.322e+06   0.000   1.0000
Year2009     6.714e+01  7.322e+06   0.000   1.0000
Year2010     6.880e+01  7.322e+06   0.000   1.0000
Year2011     6.965e+01  7.322e+06   0.000   1.0000
Year2012     6.833e+01  7.322e+06   0.000   1.0000
Year2013     6.900e+01  7.322e+06   0.000   1.0000
Year2014     6.962e+01  7.322e+06   0.000   1.0000
Year2015     6.698e+01  7.322e+06   0.000   1.0000
Year2016     6.750e+01  7.322e+06   0.000   1.0000
Year2017     6.789e+01  7.322e+06   0.000   1.0000
SurveyGHL   -1.399e+00  5.476e-01  -2.555   0.0106 *
SurveySF    -1.627e+00  3.284e-01  -4.955 7.24e-07 ***
---
Signif. codes:  0 *** 0.001 ** 0.01 * 0.05 . 0.1   1

Approximate significance of smooth terms:
             edf Ref.df Chi.sq  p-value
s(Axis_km) 17.99  21.95 186.95  < 2e-16 ***
s(Depth_m)  1.00   1.00  30.15 3.99e-08 ***
---
Signif. codes:  0 *** 0.001 ** 0.01 * 0.05 . 0.1   1

R-sq.(adj) =  0.0805   Deviance explained = 87.8%
-REML = 625.14  Scale est. = 1         n = 10373

Family: Negative Binomial(1.125)
Link function: log

Formula:
Number_Tusk ~ offset(log(Sweptarea_km2)) + s(Axis_km, k = 100) +
    s(Depth_m, k = 5) + s(DayOfYear, bs = "cc", k = 5) + s(Time,
    bs = "cc", k = 5) + Year + Survey

Parametric coefficients:
              Estimate Std. Error z value Pr(>|z|)
(Intercept) -7.1232930  2.8343537  -2.513 0.011964 *
Year1982    -1.1367712  0.3635122  -3.127 0.001765 **
Year1983    -0.6406824  0.2948279  -2.173 0.029775 *
Year1984    -0.8988722  0.3560686  -2.524 0.011588 *
Year1985    -0.0581976  0.2420223  -0.240 0.809971
Year1986    -0.0005265  0.2933307  -0.002 0.998568
Year1987     0.1042070  0.3100971   0.336 0.736836
Year1988    -0.4420938  0.3164222  -1.397 0.162364
Year1989    -1.1551186  0.3543822  -3.260 0.001116 **
Year1990    -1.1821534  0.3562974  -3.318 0.000907 ***
Year1991    -1.5624830  0.3409467  -4.583 4.59e-06 ***
Year1993    -1.0290328  0.3973669  -2.590 0.009608 **
Year1995    -2.4544204  0.6043209  -4.061 4.88e-05 ***
Year1996    -1.3395964  0.4315131  -3.104 0.001907 **
Year1997    -1.8353520  0.4753399  -3.861 0.000113 ***
Year1998    -1.7753546  0.4423085  -4.014 5.97e-05 ***
Year1999    -2.1379331  0.5158502  -4.144 3.41e-05 ***
Year2000    -1.3484051  0.3970787  -3.396 0.000684 ***
```

```
Year2001    -0.8559063  0.3068099  -2.790 0.005276 **
Year2002    -0.1095745  0.3030086  -0.362 0.717635
Year2003     0.2221433  0.2663153   0.834 0.404204
Year2004     0.1624467  0.2787079   0.583 0.559990
Year2005     0.4649899  0.2639624   1.762 0.078141 .
Year2006     0.4652988  0.2716828   1.713 0.086776 .
Year2007     0.5552471  0.2637340   2.105 0.035263 *
Year2008     0.4256415  0.2650679   1.606 0.108322
Year2009     0.6840428  0.2585006   2.646 0.008140 **
Year2010     0.7215463  0.2561974   2.816 0.004857 **
Year2011     0.5506166  0.2552551   2.157 0.030996 *
Year2012     0.5836856  0.2573362   2.268 0.023318 *
Year2013     1.1014842  0.2495653   4.414 1.02e-05 ***
Year2014     0.7341741  0.2509891   2.925 0.003443 **
Year2015     0.8181581  0.2485972   3.291 0.000998 ***
Year2016     1.1196989  0.2391143   4.683 2.83e-06 ***
Year2017     0.4910285  0.2717676   1.807 0.070794 .
SurveyGHL   -0.7663322  0.2388948  -3.208 0.001337 **
SurveySF    -0.1973901  0.1979553  -0.997 0.318694
---
Signif. codes:  0 *** 0.001 ** 0.01 * 0.05 . 0.1   1

Approximate significance of smooth terms:
                       edf Ref.df Chi.sq  p-value
s(Axis_km)          38.487 46.297 659.63  < 2e-16 ***
s(Depth_m)           3.945  3.996 647.17  < 2e-16 ***
s(DayOfYear)         1.955  3.000  19.65 1.12e-05 ***
s(Time)  2.196  3.000  15.26 0.000259 ***
---
Signif. codes:  0 *** 0.001 ** 0.01 * 0.05 . 0.1   1

R-sq.(adj) =  0.423   Deviance explained = 62.8%
-REML = 3940.5  Scale est. = 1         n = 10373
```